

REACTIONAL TORQUE OF LINEAR RADIATORS

A Thesis Presented to
The Faculty of Graduate Studies
of
The University of Manitoba

In Partial Fulfilment of the
Requirements for the Degree of
Master of Science in Electrical Engineering

Jane Dobrovolny

September 1973



ABSTRACT

A theoretical investigation is made of the relation between radiated power and reactional torque of both infinitely long line sources and dipole antennas. Since the reactional torque is caused by interaction between at least two sources, arrangements of two line sources or two dipoles are usually considered. The advantage of adding more sources to the configuration is discussed. A possible influence of a supporting structure approximated by a circular cylinder is examined. Comparison is made between the torque efficiency of antennas close to a conducting cylinder and the torque efficiency of antennas close to a dielectric cylinder. Lastly, it is shown that a three dipole turnstile antenna can be used to produce torque in an arbitrary direction.

ACKNOWLEDGEMENT

The author wishes to thank Dr. L. Shafai who suggested this problem and gave her help and encouragement during this investigation.

LIST OF SYMBOLS

A	surface
\bar{A}	magnetic potential
\bar{a}_r	
\bar{a}_z	unit vectors in r, z and ρ direction, respectively
\bar{a}_ρ	
\bar{B}	magnetic field density
b	distance of source from the origin
\bar{D}	electric field density
d	direct distance between two sources
\bar{E}	electric field intensity
\bar{F}	force
\bar{G}	linear momentum
\bar{H}	magnetic field intensity
I	current
\bar{I}	unit second rank tensor
\bar{J}	current density
k	wave number
\bar{L}	angular momentum
\bar{T}	torque
t	time
V	volume
α	eigenvalue in z - direction
γ	phase difference between two sources

ϵ_0 permittivity of free space
 ϵ_d permittivity of a dielectric
 μ_0 permeability of free space
 σ volume charge distribution
 ϕ_0 spacial angle between two sources
 ψ wave function
 ω frequency

LIST OF FIGURES

Fig. 1 - Space vehicle with a turnstile antenna 4

Fig. 2 - Arrangement of two line sources close
to a cylinder 6

Fig. 3 - Arrangement of two dipoles close to a
cylinder 6

Fig. 4 - A current filament in free space 15

Fig. 5 - Two current filaments in free space 17

Fig. 6 - Illustration of the arrangement of two
line sources 24

Fig. 7 - Torque/power ratio of two line sources
in free space 25

Fig. 8 - Torque/power ratio of two line sources
in free space 26

Fig. 9 - Maximum torque/power ratio of two line
sources in free space as compared to the
case in which a conducting cylinder is
present 27

Fig.10 - Torque 28

Fig.11 - Reactional torque of two line sources in
free space 30

Fig.12 - Reactional torque of two line sources in
free space 31

Fig.13 - Reactional torque of two line sources in free space	32
Fig.14 - Line sources equispaced on surface of a cylinder	34
Fig.15 - Configuration of three line sources in free space	37
Fig.16 - Configuration of four line sources in free space	43
Fig.17 - Torque/power ratio of two, three and four sources configurations in free space	45
Fig.18 - Arrangement of two line sources close to a conducting cylinder	47
Fig.19 - Power radiated by two line sources close to a cylinder	52
Fig.20 - Torque/power ratio of two line sources close to a conducting cylinder	53
Fig.21 - Torque/power ratio of two line sources close to a conducting cylinder	54
Fig.22 - Torque/power ratio of two line sources close to a conducting cylinder	55
Fig.23 - Torque/power ratio of two line sources close to a conducting cylinder	56
Fig.24 - Reactional torque of two line sources close to a conducting cylinder	57

Fig.25 - Torque/power ratio of two line sources close to a conducting cylinder; cylinder radius is the independent variable	58
Fig.26 - Torque of two line sources close to a conducting cylinder; cylinder radius is the independent variable	59
Fig.27 - Arrangement of two line sources close to a dielectreic cylinder	61
Fig.28 - Torque/power ratio of two line sources close to a dielectric cylinder	66
Fig.29 - Torque/power ratio of two line sources close to a dielectric cylinder	67
Fig.30 - Torque/power ratio of two line sources close to a dielectric cylinder	68
Fig.31 - Arrangement of two dipoles close to a conducting cylinder	71
Fig.32 - Contour of integration in α -plane	76
Fig.33 - Contour of integration in χ -plane	76
Fig.34 - Power radiated by two dipoles close to a conducting cylinder	86
Fig.35 - Torque/power ratio of two dipoles close to a conducting cylinder	87
Fig.36 - Torque/power ratio of two dipoles close to a conducting cylinder	88

Fig.37 - Turnstile antenna	90
Fig.38 - Three crossed dipoles	90

TABLE OF CONTENTS

ABSTRACT i
ACKNOWLEDGEMENTS ii
LIST OF SYMBOLS iii
LIST OF FIGURES v
TABLE OF CONTENTS ix
I. INTRODUCTION 1
II. REACTIONAL TORQUE OF ELECTROMAGNETIC FIELDS 8
III. TWO - DIMENSIONAL RADIATION 14
III - 1. Radiation of a line source 15
III - 2. Two line sources 17
III - 3. Line sources equispaced on surface of a cylinder 34
III - 3.1. Three line sources 37
III - 3.2. Four line sources 42
IV. LINE SOURCES IN THE PRESENCE OF A CYLINDER 47
IV - 1. Line sources and an infinite conducting cylinder.. 48
IV - 2. Line sources and an infinite dielectric cylinder.. 61
V. DIPOLES IN THE PRESENCE OF AN INFINITE CONDUCTING
CYLINDER 70
VI. TORQUE IN AN ARBITRARY DIRECTION 89
APPENDIX 101
REFERENCES 106

I. INTRODUCTION

In 1873 J. C. Maxwell stated the theory of radiation pressure in the form which is used today. Dealing with the stresses in electromagnetic fields, he arrived at the conclusion that "... in a medium in which waves are propagated there is a pressure in the direction normal to the waves, and numerically equal to the energy in unit of volume." For strong sunlight Maxwell gives the estimation of 0.000 000 088 2 lb/ft². (1)

This value had been generally considered too small to be detected experimentally. To those who attempted, the main obstacles encountered during the measurements were disturbances due to temperature differences between the body the radiation was to act upon and its surroundings. At the turn of the century and especially later in 1930's, several successful experiments were performed corroborating Maxwell's statement.

Peter Lebedev (1901)⁽²⁾ "qualitatively" confirmed the expression given by Maxwell and Bartoli for light pressure of reflected rays

$$p = \frac{E}{c}(1+\rho)$$

where E is the energy received per second, c the velocity of light and ρ the reflectivity power of the surface that varies from 0 for a black surface to 1 for a perfectly reflecting one. Similar results were obtained also by E. F. Nichols and G. F. Hull⁽³⁾ in 1902.

A slightly different approach was employed by R. A. Beth⁽⁴⁾ in 1935. He used a beam of elliptically polarized light incident on a doubly refracting plate that altered its polarization into a linear one. In this set up, the direction of the electric field was no longer parallel to the electric displacement vector and hence was not perpendicular to the direction of propagation in the crystal, which resulted in a torque on the plate.

In the theoretical work accompanying the above mentioned experiments, it has been affirmed that torque is inversely proportional to the frequency used. It is therefore understandable, that although most of the experiments were done at visible light frequencies, the first attempts to employ radiation pressure were for centimeter waves. In 1949 N. Carrara and P. Lombardini⁽⁹⁾ reported measurements of torque at 3.2 cm wavelength using 50 W mean power. Torque was of the order of 10^{-3} dyne-cm as was expected, but apart from this more exact results were not obtained. Independent

of them, A. L. Cullen⁽⁵⁾ did similar experiments and went even further by proposing a method of measuring power at microwave frequencies using radiation pressure. The error of his wattmeter was estimated to be ± 0.6 W at the 25 W level, depending on determination of mechanical constants of the system.

In the earth-bound experiments, however, the possibilities of utilizing radiation pressure (besides the power measurements in the waveguides) were limited by its small values as compared to the effects of the atmosphere. With the beginning of spaceflights, the question of the momentum possessed by electromagnetic waves again became popular. In 1963 a theoretical investigation was made of the reactional torque on radiating dipole antennas. The possibilities of using it to stabilize a space vehicle were suggested by P. Brusaglioni, A. Consortini and G. Toraldo di Francia⁽⁶⁾. They considered three ways of applying electromagnetic radiation to the spaceship:

- a) the antenna is placed on the vehicle and radiates elliptically polarized waves
- b) the antenna situated on the vehicle is receiving radiation from a ground station
- c) the torque is caused by simultaneous radiation by both the ground antenna and the vehicle antenna.

They showed that while the first method produces adequate

torque to offset the usual disturbances in space using reasonable power (about 5 kW), the other two methods would need more than 10^5 kW to achieve the same result.

In 1966 reactional torque was experimentally demonstrated on a loop torque-antenna by F. S. Chute⁽⁷⁾. The difference between the theoretical estimation and the actual torque obtained was about 20%, which could be attributed to the approximations in the theory inasmuch as coarseness of the experiment.

The preceding experiments and proposals had one thing in common; they all dealt with an antenna located in free space⁽⁷⁾, or as in the work of P. Bruscallioni, A. Consortini and G. Toraldo di Francia, with turnstile antenna dimensions much larger than the space vehicle on which it was mounted. (See fig. 1)

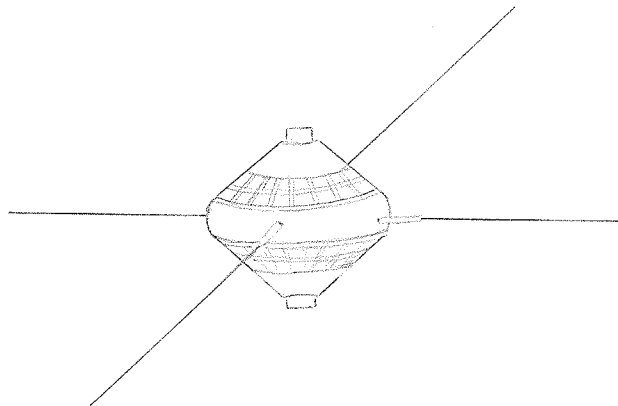


Fig. 1 - Space vehicle with a turnstile antenna⁽⁶⁾

It may be of practical interest to examine the behaviour of antennas mounted on vehicles of comparable or larger size. As a starting point in chapter III, two infinitely long line sources are chosen, allowing us to reduce the problem to two dimensions. The second part of this chapter expands the problem to a larger number of line sources evenly distributed on a cylindrical surface. The respective power and torque relations are examined and compared. Since the power is not constant for the individual configurations, the relative value of torque/power ratio is always calculated.

In chapter IV, to simulate the presence of the spaceship, either a conducting or a dielectric cylinder is added to the configuration of two line sources (fig. 2). Both the power and the torque efficiency can thus be increased or decreased, depending on the spacial angle and the length of the holding arms of the antennas.

In chapter V the next step is taken to consider dipoles close to a cylinder of great length (fig. 3). This is a more practical case since many spaceships are using dipole antennas for various purposes. If the cylinder is removed this configuration is identical with a beam radiator described by Chute⁽⁷⁾. (Appendix)

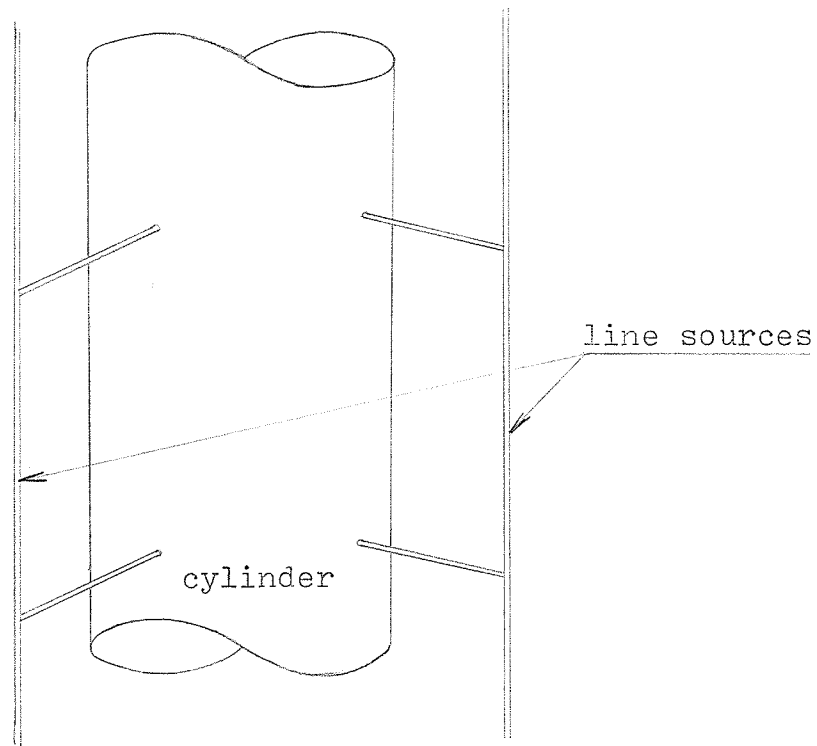


Fig. 2 - Arrangement of two line sources close to a cylinder

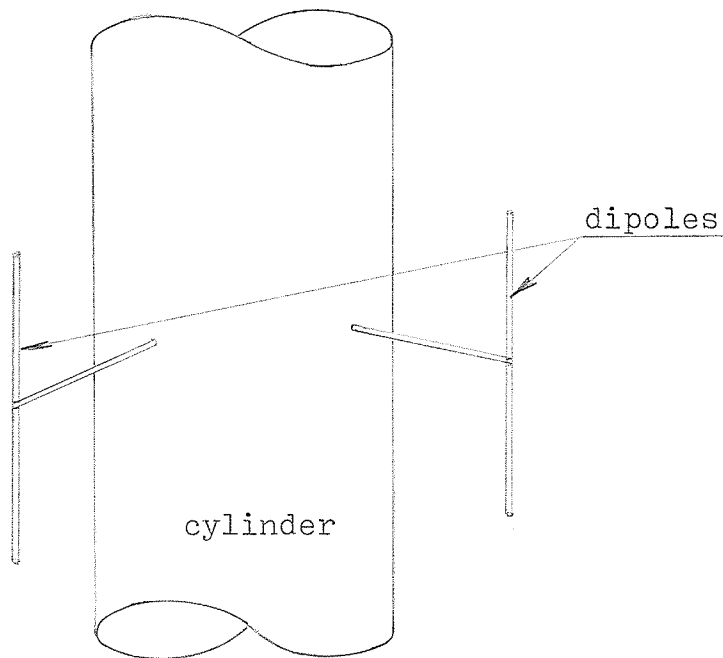


Fig. 3 - Arrangement of two dipoles close to a cylinder

The possibility of producing torque about an arbitrary axis is the topic of chapter VI. The turnstile antenna described by Chute⁽⁷⁾ and P. Brusaglioni, A. Consortini and G. Toraldo di Francia⁽⁶⁾ is modified by the addition of a third dipole. The desired direction of torque is obtained by varying the phases of the dipoles.

II. REACTIONAL TORQUE OF ELECTROMAGNETIC FIELDS

"To every action there is always opposed an equal reaction" states Newton's third law of motion. In other words, bringing it closer to our problem, the energy that is radiated by an antenna is counterbalanced by a reactive force acting on the antenna.

Before we can proceed to consider concrete arrangements of the antennas, it would be useful to develop and clarify the concept of a reactional torque. In general, the radiation pressure (or force) is directly linked to the linear momentum flow exhibited by the electromagnetic waves:

$$\bar{F} = \frac{d\bar{G}_{\text{mech}}}{dt} \quad (1)$$

where \bar{F} is the force,

\bar{G} is the linear momentum

and t is time.

Similarly the torque \bar{T} is associated with the angular momentum \bar{L} through the relationship

$$\bar{T} = \frac{d\bar{L}_{\text{mech}}}{dt} \quad (2)$$

Let us first consider volume charge and current distributions in an external electromagnetic field. The total

force on all the particles throughout the volume V is:

$$\bar{F} = \int_V [\bar{\sigma} \bar{E} + (\bar{J} \times \bar{B})] dV \quad (3)$$

\bar{E} is the electric field intensity,

\bar{B} is the magnetic field density,

the volume charge distribution is $\bar{\sigma} = \text{div } \bar{D}$ (4)

and the current distribution is $\bar{J} = \text{curl } \bar{H} - \frac{\delta \bar{D}}{\delta t}$ (5)

In the equations (4) and (5)

\bar{H} is the magnetic field intensity

\bar{D} is the electric field density

Substituting (1), (4) and (5) into (3) gives

$$\frac{d\bar{G}_{\text{mech}}}{dt} = \int_V (\bar{E} \cdot \text{div } \bar{D} - \bar{B} \times \text{curl } \bar{H} + \bar{B} \times \frac{\delta \bar{D}}{\delta t}) dV \quad (6)$$

Then writing

$$\bar{B} \times \frac{\delta \bar{D}}{\delta t} = \frac{\delta}{\delta t} (\bar{B} \times \bar{D}) + \bar{D} \times \frac{\delta \bar{B}}{\delta t}$$

it becomes

$$\frac{d\bar{G}_{\text{mech}}}{dt} + \int_V \frac{\delta}{\delta t} (\bar{D} \times \bar{B}) dV = \int_V (\bar{E} \cdot \text{div } \bar{D} - \bar{B} \times \text{curl } \bar{H} - \bar{D} \times \text{curl } \bar{B}) dV \quad (7)$$

The integrand on the righthand side of the equation (7) can be identified as a divergence of the Maxwell stress tensor:

$$\vec{S} = \vec{H} \cdot \vec{B} + \vec{E} \cdot \vec{D} - \frac{1}{2} \vec{I} \cdot (\vec{E} \cdot \vec{D} + \vec{H} \cdot \vec{B}) \quad (8)$$

(\vec{I} is defined as a unit second rank tensor)

Therefore

$$\frac{d\bar{G}_{\text{mech}}}{dt} + \int_V \frac{\delta}{\delta t} (\vec{D} \times \vec{B}) \cdot dV = \int_V \text{div } \vec{S} \cdot dV$$

Now

$$\int_V \text{div } \vec{S} \cdot dV = \oint_A \vec{S} \cdot \vec{n} \cdot dA$$

where A is a closed surface that encloses the volume V.

The integration and derivation on the lefthand side of equation (7) are interchangeable in the fixed frame of reference:

$$\int_V \frac{\delta}{\delta t} (\vec{D} \times \vec{B}) \cdot dV = \frac{\delta}{\delta t} \int_V (\vec{D} \times \vec{B}) \cdot dV$$

Substituting back we obtain:

$$\frac{d\bar{G}_{\text{mech}}}{dt} + \frac{\delta}{\delta t} \int_V (\vec{D} \times \vec{B}) \cdot dV = \oint_A \vec{S} \cdot \vec{n} \cdot dA \quad (9)$$

This is the law of conservation of linear momentum.

The angular momentum may also be defined as "the moment of linear momentum":

$$\bar{L} = \bar{r} \times \bar{G}_{\text{mech}} \quad (10)$$

where \bar{r} is the position vector of the point in which the angular momentum with respect to the origin is calculated. Accordingly the law of conservation of angular momentum has the form

$$\frac{d}{dt}(\bar{r} \times \bar{G}_{\text{mech}}) + \frac{\delta}{\delta t} \int_V \bar{r} \times (\bar{D} \times \bar{B}) dV = \oint_A \bar{r} \times \bar{S} \cdot \bar{n} dA$$

Since

$$\frac{d}{dt}(\bar{r} \times \bar{G}_{\text{mech}}) = \frac{d\bar{L}}{dt} = \bar{T} \quad (11)$$

it follows that

$$\bar{T} = \oint_A \bar{r} \times \bar{S} \cdot \bar{n} dA - \frac{\delta}{\delta t} \int_V \bar{r} \times (\bar{D} \times \bar{B}) dV \quad (12)$$

We are interested in the steady state mechanical reaction on the radiating source. Consequently from the steady state conditions the time average of

$$\frac{\delta}{\delta t} \int_V \bar{r} \times (\bar{D} \times \bar{B}) dV$$

is zero.

Hence the real time averaged torque exerted on the antenna is:

$$\bar{T}_{av} = \frac{1}{2} \operatorname{Re} \oint_A \bar{\mathbf{r}} \times \bar{\mathbf{S}}^* \cdot \bar{\mathbf{n}} \, dA \quad (13)$$

where * denotes the conjugate.

Expression $\bar{\mathbf{S}} \cdot \bar{\mathbf{n}}$ may be considered as a stress transmitted across the surface of normal $\bar{\mathbf{n}}$. Stratton⁽⁸⁾ proves that

$$\bar{\mathbf{S}} \cdot \bar{\mathbf{n}} = \epsilon_0 (\bar{\mathbf{E}} \cdot \bar{\mathbf{n}}) \cdot \bar{\mathbf{E}} - \frac{\epsilon_0}{2} \bar{\mathbf{E}}^2 \cdot \bar{\mathbf{n}} + \frac{1}{\mu_0} (\bar{\mathbf{B}} \cdot \bar{\mathbf{n}}) \cdot \bar{\mathbf{B}} - \frac{1}{2\mu_0} \bar{\mathbf{B}}^2 \cdot \bar{\mathbf{n}} \quad (14)$$

If $\bar{\mathbf{E}}$ and $\bar{\mathbf{B}}$ are oscillating functions, the time average of $\bar{\mathbf{S}} \cdot \bar{\mathbf{n}} = \frac{1}{2} \bar{\mathbf{S}}^* \cdot \bar{\mathbf{n}}$ and eq. (13) can be rewritten as

$$\bar{T} = \frac{1}{2} \operatorname{Re} \oint_A \bar{\mathbf{r}} \times \left[\epsilon_0 (\bar{\mathbf{E}}^* \cdot \bar{\mathbf{n}}) \cdot \bar{\mathbf{E}} - \frac{\epsilon_0}{2} \bar{\mathbf{E}}^2 \cdot \bar{\mathbf{n}} + \frac{1}{\mu_0} (\bar{\mathbf{B}}^* \cdot \bar{\mathbf{n}}) \cdot \bar{\mathbf{B}} - \frac{1}{2\mu_0} \bar{\mathbf{B}}^2 \cdot \bar{\mathbf{n}} \right] dA \quad (15)$$

In the above expression the integration is taken over any closed surface A. Let A be a spherical surface extending to infinity, then $\bar{\mathbf{r}}$ and $\bar{\mathbf{n}}$ have the same direction. \bar{T} is reduced to

$$\bar{T} = \frac{1}{2} \operatorname{Re} \oint_A \bar{\mathbf{r}} \times \left[\epsilon_0 (\bar{\mathbf{E}}^* \cdot \bar{\mathbf{n}}) \cdot \bar{\mathbf{E}} + \frac{1}{\mu_0} (\bar{\mathbf{B}}^* \cdot \bar{\mathbf{n}}) \cdot \bar{\mathbf{B}} \right] dA \quad (16)$$

In many of the following cases the surface of the integration A_c is going to be cylindrical. The final form of the result is identical with (16), only \bar{n} and \bar{r} are replaced by \bar{a}_ρ and $\bar{\rho}$, respectively, and we get

$$\bar{T} = \frac{1}{2} \operatorname{Re} \int_{A_c} \bar{\rho} \times [\epsilon_0 (\bar{E}^* \cdot \bar{a}_\rho) \cdot \bar{E} + \frac{1}{\mu_0} (\bar{B}^* \cdot \bar{a}_\rho) \cdot \bar{B}] dA_c \quad (17)$$

Generally the power radiated is

$$P = \frac{1}{2} \operatorname{Re} \oint_A (\bar{E} \times \bar{H}^*) \cdot \bar{n} dA \quad (18)$$

For the spherical surface $\bar{n} = \bar{a}_r$ and for the cylindrical surface $\bar{n} = \bar{a}_\rho$.

Equations (16), (17) and (18) will enable us to find the torque and the power required to produce it, once the radiated fields are known. In the following chapters attention is paid primarily to derive the fields and then, using the above equations, to calculate the torque, power and their ratio.

III. TWO - DIMENSIONAL RADIATION

There has been a great deal of attention concentrated on investigation of torque due to two radiating dipoles^{(6),(7)} while the line sources were not discussed as often. It seems to be an advantage to include the two, three and four line sources configurations into the topic of this paper, as it will make the interactions between the individual sources that cause torque more apparent.

The line sources are assumed to be parallel with the z - axis in our system of coordinates; the current distributions along the lines are uniform, i.e. do not depend on z . For this reason the problem is reduced to a two - dimensional one. In the following, first fields of one line source are derived and the result is used to obtain the reactional torque and power of two line sources configuration. The third part of this section then generalizes the problem for any number of line sources equispaced on a cylindrical surface.

III - 1. Radiation field of a line source

The line source is located at point P (fig. 4). Its position is given by b and ϕ_0 . The current distribution has magnitude I and changes sinusoidally with time at a frequency ω . The radiation field is given by the wave function (10)

$$\psi = \frac{I}{4i} H_0^{(2)}(k|\rho - b|) \quad (19)$$

or using the addition theorem for Hankel functions it becomes

$$\psi = \begin{cases} \frac{I}{4i} \sum_{n=-\infty}^{\infty} H_n^{(2)}(kb) J_n(k\rho) \exp[in(\phi - \phi_0)] & \rho < b \\ \frac{I}{4i} \sum_{n=-\infty}^{\infty} J_n(kb) H_n^{(2)}(k\rho) \exp[in(\phi - \phi_0)] & \rho > b \end{cases} \quad (20)$$

where $H_n^{(2)}$ is the Hankel function of the second kind of order n and J_n is the Bessel function.

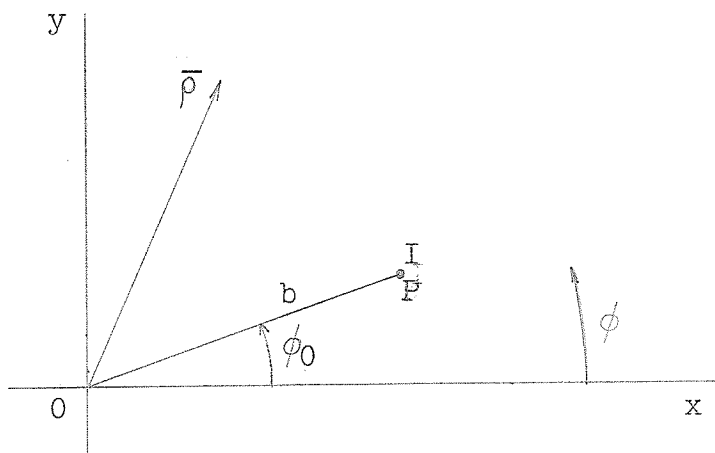


Fig. 4 - A current filament in free space

The corresponding electromagnetic fields are then

$$E_\rho = E_\phi = H_z = 0$$

$$E_z = \frac{k^2 \psi}{ie_0 \omega} = \begin{cases} -\frac{k^2 I}{4e_0 \omega} \sum_{n=-\infty}^{\infty} H_n^{(2)}(kb) J_n(k\rho) \exp[in(\phi - \phi_0)] & \rho < b \\ -\frac{k^2 I}{4e_0 \omega} \sum_{n=-\infty}^{\infty} J_n(kb) H_n^{(2)}(k\rho) \exp[in(\phi - \phi_0)] & \rho > b \end{cases} \quad (21)$$

$$H_\rho = \frac{\delta \psi}{\rho \delta \phi} = \begin{cases} \frac{I}{4\rho} \sum_{n=-\infty}^{\infty} n H_n^{(2)}(kb) J_n(k\rho) \exp[in(\phi - \phi_0)] & \rho < b \\ \frac{I}{4\rho} \sum_{n=-\infty}^{\infty} n J_n(kb) H_n^{(2)}(k\rho) \exp[in(\phi - \phi_0)] & \rho > b \end{cases} \quad (22)$$

$$H_\phi = -\frac{\delta \psi}{\delta \rho} = \begin{cases} -\frac{kI}{4i} \sum_{n=-\infty}^{\infty} H_n^{(2)}(kb) J_n'(k\rho) \exp[in(\phi - \phi_0)] & \rho < b \\ -\frac{kI}{4i} \sum_{n=-\infty}^{\infty} J_n(kb) H_n^{(2)'}(k\rho) \exp[in(\phi - \phi_0)] & \rho > b \end{cases} \quad (23)$$

where $J_n'(k\rho)$ and $H_n^{(2)'}(k\rho)$ denote the derivatives with respect to the argument of the Bessel and Hankel functions, respectively.

To produce torque at least two line sources are necessary. Thus we proceed to find the field components due to two line sources.

III - 2. Two line sources

Consider now two line sources positioned as shown in fig. 5. The sources are assumed to be infinitely long and infinitely thin uniform filaments positioned at a distance b from the point of reference. Let us further assume that they are held in place by the supporting arms that are firmly fixed in their mutual position but can freely rotate about the axis going through the point of reference and parallel to the line sources. Finally it is assumed that these supporting arms do not influence the resulting fields; i.e. reflection from them is negligible. The currents I_1 and I_2 are equal in magnitude but have a phase difference γ .

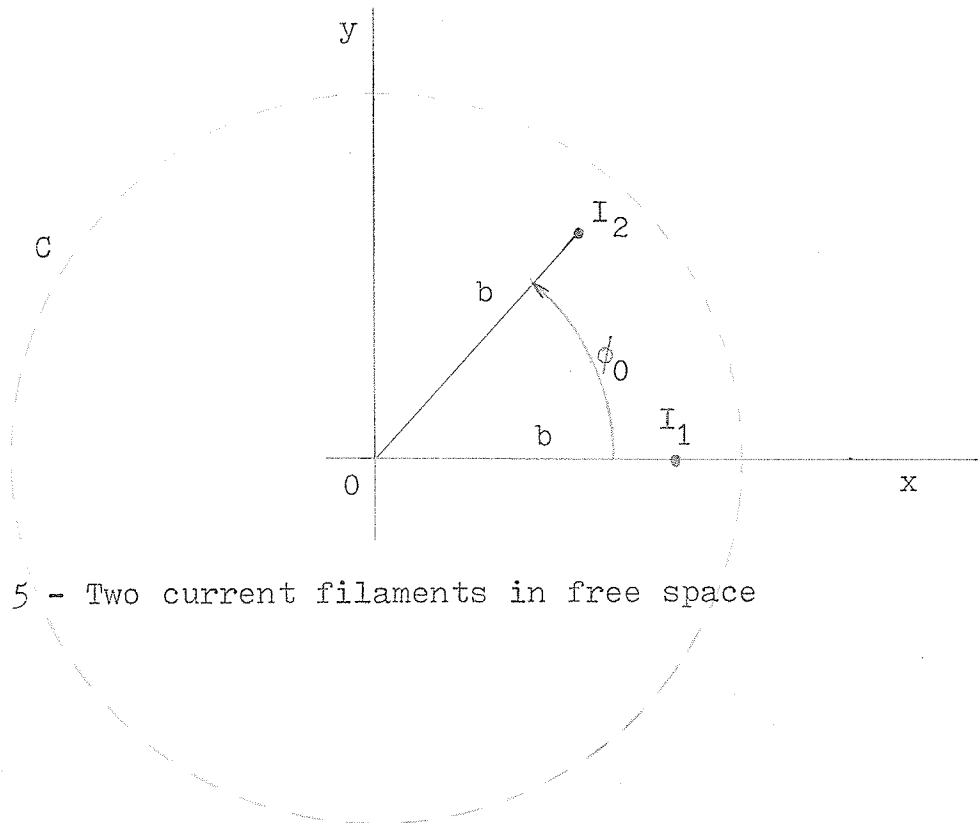


Fig. 5 - Two current filaments in free space

$$I_1 = I$$

$$I_2 = I \exp(i\gamma)$$

The total wave function is given by a linear superposition of the individual ones in the form:

$$\Psi_{\text{total}} = \Psi_1 + \Psi_2 = \begin{cases} \frac{I}{4i} \sum_{n=-\infty}^{\infty} H_n^{(2)}(kb) J_n(k\rho) \exp(in\phi) [1 + \exp(i\gamma - in\phi_0)] & \rho < b \\ \frac{I}{4i} \sum_{n=-\infty}^{\infty} J_n(kb) H_n^{(2)}(k\rho) \exp(in\phi) [1 + \exp(i\gamma - in\phi_0)] & \rho > b \end{cases} \quad (24)$$

Similarly the field components are given by:

$$E_z = E_{z1} + E_{z2} = \begin{cases} -\frac{k^2 I}{4\epsilon_0 \omega} \sum_{n=-\infty}^{\infty} H_n^{(2)}(kb) J_n(k\rho) \exp(in\phi) [1 + \exp(i\gamma - in\phi_0)] & \rho < b \\ -\frac{k^2 I}{4\epsilon_0 \omega} \sum_{n=-\infty}^{\infty} J_n(kb) H_n^{(2)}(k\rho) \exp(in\phi) [1 + \exp(i\gamma - in\phi_0)] & \rho > b \end{cases} \quad (25a)$$

$$H_{\rho} = H_{\rho 1} + H_{\rho 2} = \begin{cases} \frac{I}{4\rho} \sum_{n=-\infty}^{\infty} n H_n^{(2)}(kb) J_n(k\rho) \exp(in\phi) [1 + \\ + \exp(i\gamma - in\phi_0)] & \rho < b \\ \frac{I}{4\rho} \sum_{n=-\infty}^{\infty} n J_n(kb) H_n^{(2)}(k\rho) \exp(in\phi) [1 + \\ + \exp(i\gamma - in\phi_0)] & \rho > b \end{cases} \quad (25b)$$

$$H_{\phi} = H_{\phi 1} + H_{\phi 2} = \begin{cases} -\frac{kI}{4i} \sum_{n=-\infty}^{\infty} H_n^{(2)}(kb) J_n'(k\rho) \exp(in\phi) [1 + \\ + \exp(i\gamma - in\phi_0)] & \rho < b \\ -\frac{kI}{4i} \sum_{n=-\infty}^{\infty} J_n(kb) H_n^{(2)'}(k\rho) \exp(in\phi) [1 + \\ + \exp(i\gamma - in\phi_0)] & \rho > b \end{cases} \quad (25c)$$

In carrying out the integration indicated in Sec. II eq. (17), the cylindrical surface A_c degenerates to a closed contour C in the $x - y$ plane and the torque per unit length is then understood. The contour C , as indicated in fig. 5 is a circle about the origin and has a radius ρ . The limits of integration are obviously 0 and 2π . The equation for torque is now

$$\bar{T} = \frac{1}{2} \operatorname{Re} \int_0^{2\pi} \bar{\rho} \times \left[\epsilon_0 (\bar{E}^* \cdot \bar{a}) \cdot \bar{E} + \frac{1}{\mu_0} (\bar{B}^* \cdot \bar{a}) \cdot \bar{B} \right] d\phi \quad (26)$$

which further reduces to:

$$\bar{T} = \bar{a}_z \frac{\mu_0}{2} \operatorname{Re} \int_0^{2\pi} \rho^2 H_\rho^* H_\phi d\phi \quad (27)$$

(notice that the first part of the integrand of eq. (26) is 0, since $\bar{E}^* \cdot \bar{a}_\rho = E_z^* \bar{a}_z \cdot \bar{a}_\rho = 0$)

The expression for fields at $\rho > b$ has to be substituted into (27). Thus we obtain:

$$T_z = - \frac{\mu_0 k I^2 \rho}{8} \sum_{n=-\infty}^{\infty} n [J_n(kb)]^2 [1 + \cos(\gamma - n\phi_0)] \cdot \operatorname{Re} \left\{ \frac{1}{i} H_n^*(k\rho) H_n^{(2)}(k\rho) \right\} \quad (28)$$

Usage of

$$\operatorname{Re} \left\{ \frac{1}{i} H_n^{*(2)}(k\rho) H_n^{(2)}(k\rho) \right\} = - \frac{2}{\pi k \rho}$$

in equation (28) gives

$$T_z = \frac{\mu_0 I^2}{4} \sum_{n=-\infty}^{\infty} n [J_n(kb)]^2 [1 + \cos(\gamma - n\phi_0)] \quad (29)$$

or, if summation from 0 to ∞ is used

$$T_z = \frac{\mu_0 I^2}{4} \sin \gamma \sum_{n=0}^{\infty} n \epsilon_n \sin n\phi_0 [J_n(kb)]^2 \quad (30a)$$

where $\epsilon_n = 1$ for $n = 0$
 $= 2$ for $n \neq 0$

From now on symbol T instead of T_z will be used as the torque has only z-component.

The equation (29) demonstrates that the torque carried by the cylindrical waves, which are radiated by two line sources, is independent of the position at which it is calculated (provided that $\rho > b$) and is a function of the arrangement of the line sources only.

The time average power radiated per unit length by the two sources is found from eq. (18). As in the torque calculation, the integration path is along C in fig. 5. The power is

$$P = -\frac{1}{2} \operatorname{Re} \int_0^{2\pi} \rho E_z H_\rho^* d\phi \quad (31)$$

and after substitution of equations (25a) and (25b) for E_z and H_ρ and carrying out the integration it becomes:

$$P = \frac{k^3 \pi I^2 \rho}{4\epsilon_0 \omega} \operatorname{Re} \left\{ i \sum_{n=-\infty}^{\infty} [J_n(kb)]^2 [1 + \cos(\gamma - n\phi_0)] H_n^{(2)}(k\rho) \cdot H_n^*(k\rho) \right\} \quad (32)$$

Since

$$\operatorname{Re} \left\{ i H_n^{*(2)}(k\rho) H_n^{(2)}(k\rho) \right\} = \frac{2}{\pi k\rho}$$

we arrive at the expression for the power in a form

$$P = \frac{k^2 I^2}{4\epsilon_0 \omega} \sum_{n=-\infty}^{\infty} [J_n(kb)]^2 [1 + \cos(\gamma - n\phi_0)] \quad (33)$$

or, if summation from 0 to ∞ is used

$$P = \frac{k^2 I^2}{4\epsilon_0 \omega} \sum_{n=0}^{\infty} \epsilon_n [J_n(kb)]^2 [1 + \cos n\phi_0 \cos \gamma] \quad (34)$$

An additional examination of (30) shows a dependency of the torque on the phase difference γ of the two sources and their mutual position angle ϕ_0 . If both currents are in phase ($\gamma = 0$) the torque vanishes, while power will fluctuate depending on the position angle ϕ_0 :

$$P = \frac{k^2 I^2}{4\epsilon_0 \omega} \sum_{n=0}^{\infty} \epsilon_n [J_n(kb)]^2 (1 + \cos n\phi_0)$$

If both sources are brought together at the same place, $\phi_0 = 0$, and the above equation reduces to

$$P = \frac{k^2 I^2}{2\epsilon_0 \omega} = \frac{\mu_0 I^2 \omega}{2}$$

(since $\sum_{n=0}^{\infty} \epsilon_n [J_n(kb)]^2 = 1$ and $k^2 = \omega^2 \mu_0 \epsilon_0$).

This is the same as power radiated by one current filament that has current of magnitude $2I$.

Evidently from (30a) the maximum torque is obtained for $\gamma = \pi/2$. In this case

$$T = \frac{\mu_0 I^2}{4} \sum_{n=0}^{\infty} n \epsilon_n \sin n\phi_0 [J_n(kb)]^2 \quad (30b)$$

$$P = \frac{\mu_0 I^2 \omega}{4}$$

From the above equations the expression for the torque can be rewritten as

$$T = \frac{1}{\omega} P \sum_{n=0}^{\infty} n \epsilon_n \sin n\phi_0 [J_n(kb)]^2 \quad (35)$$

Assigning $M = \sum_{n=0}^{\infty} n \epsilon_n \sin n\phi_0 [J_n(kb)]^2$ we get

$$M = \omega \frac{T}{P} \quad (36)$$

Let us define d as a direct distance between the two sources. Then, from fig. 6,

$$d = 2b \sin(\phi_0/2)$$

that is:

$$\frac{d}{\lambda} = \frac{kb}{\pi} \sin(\phi_0/2) \quad (37)$$

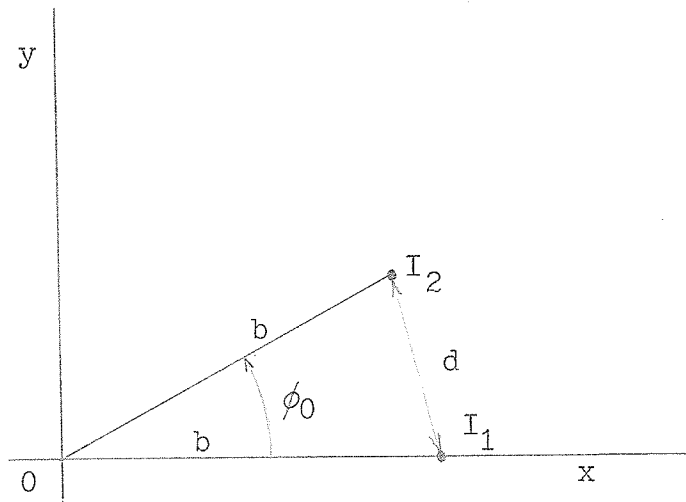


Fig. 6 - Illustration of the arrangement of two line sources

where $\lambda = 2\pi/k$ is the wavelength of the radiated field.

As we move one of the antennas around the imaginary cylindrical surface, the torque/ power ratio changes from negative to positive values almost periodically.

Taking the case of $\gamma = \pi/2$, we see that $M = 0$ for $\phi_0 = 0$

(both antennas are at the same position) and for $\phi_0 = \pi$.

At $\phi_0 = \pi$ the force which arises due to the interference between the two antennas is directed through the point of reference, causing the torque to equal zero. Fig. 7 shows torque/power vs length/wavelength dependence for different

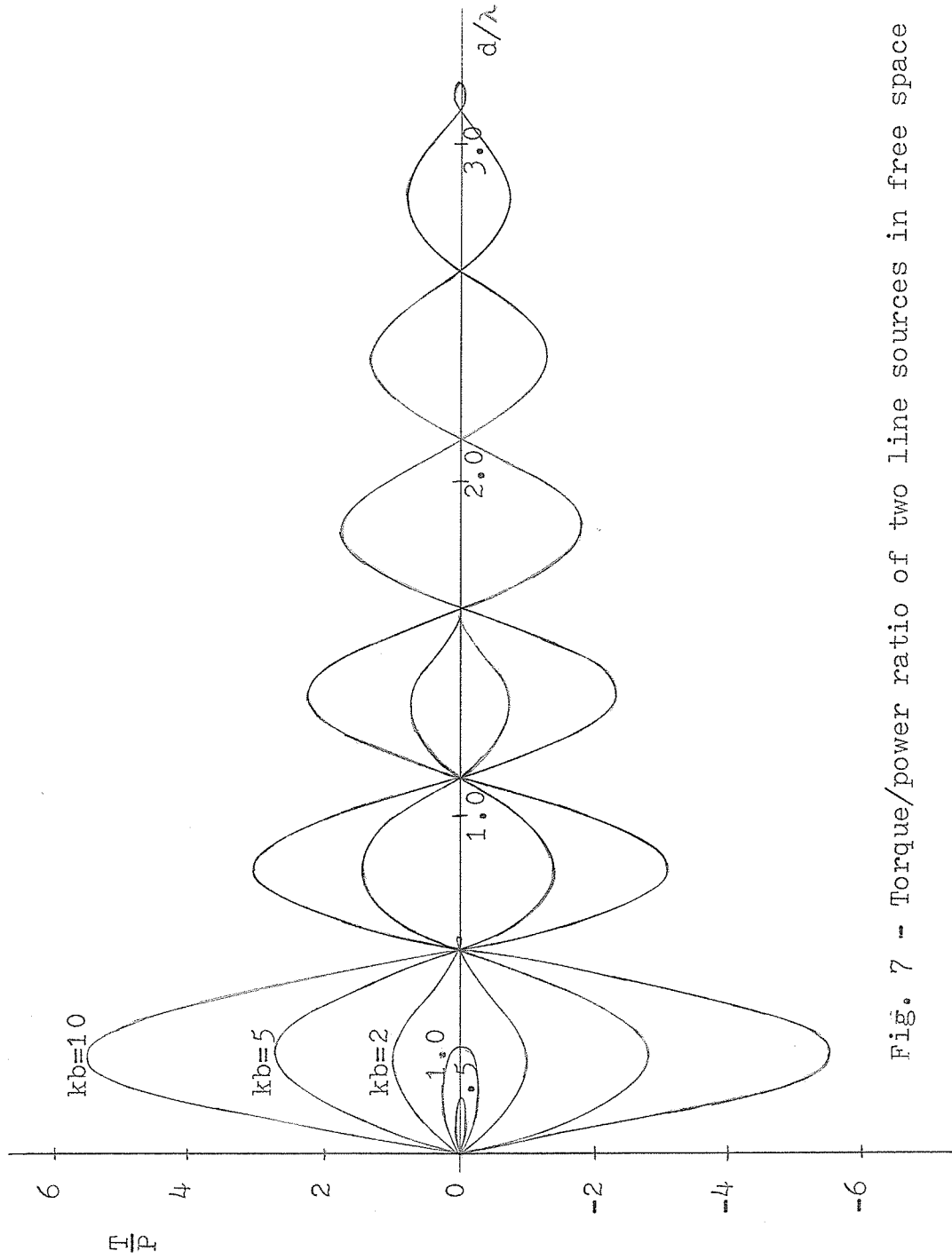


Fig. 7 - Torque/power ratio of two line sources in free space

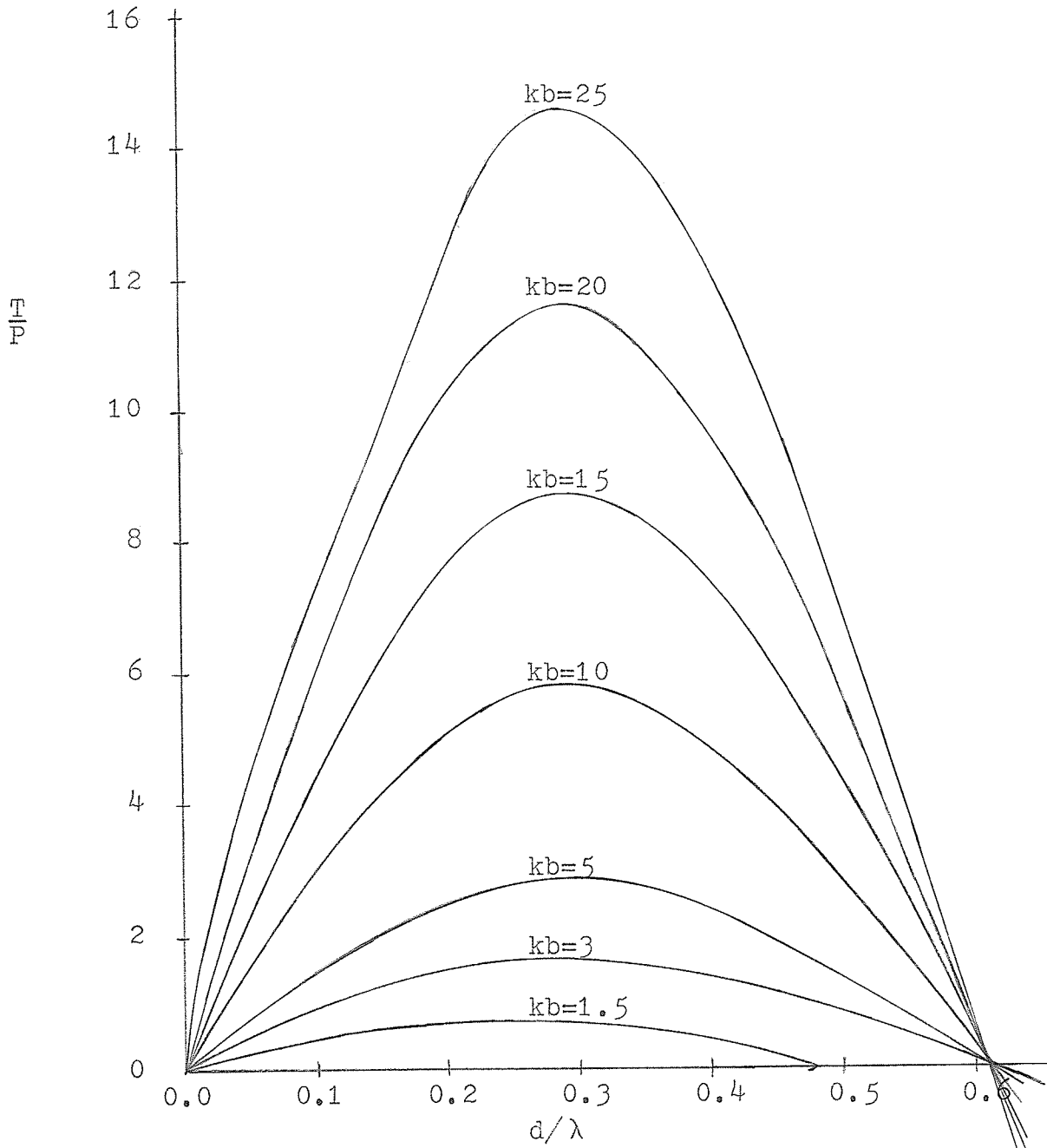


Fig. 8 - Torque/power ratio of two line sources in free space

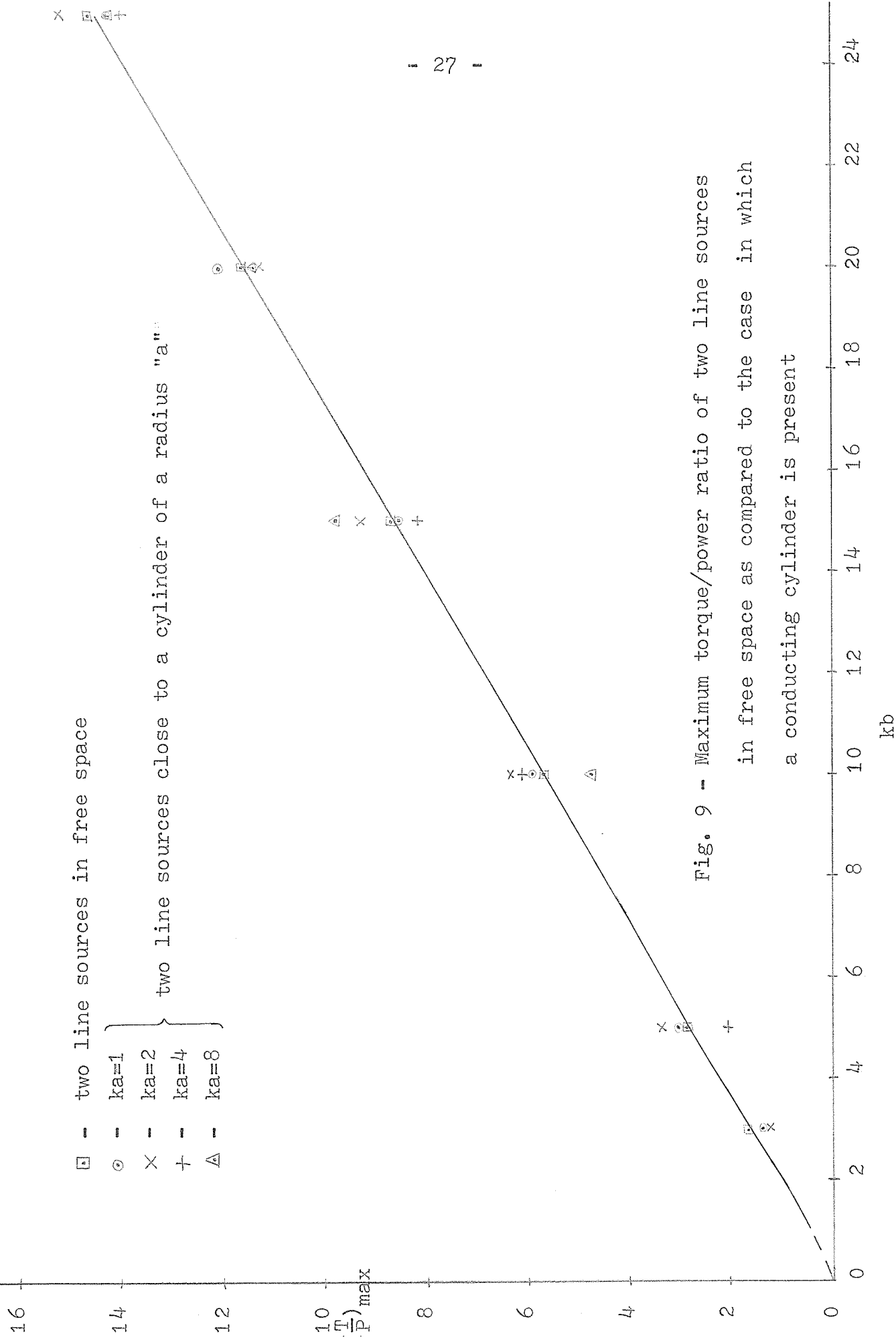


Fig. 9 - Maximum torque/power ratio of two line sources in free space as compared to the case in which a conducting cylinder is present

lengths of the holding arms. Up to $kb = 1.92$ there is only one zero crossing which is due to the above mentioned condition of $\phi_0 = \pi$. As kb increases further, the largest possible value of d/λ for given kb moves upward and the curve has 2 or more zero crossings, the first of which always occurs at $d/\lambda = 0.61$, the second at 1.12, etc. However, the peak of the curve always lies between $d/\lambda = 0$ and $d/\lambda = 0.61$. From approximately $kb = 5$ the maximum does not change the position, occurring always at $d/\lambda = 0.29$.

Generally speaking, torque is directly proportional to the length of the arm the force is acting upon:

$$T = F \cdot b$$

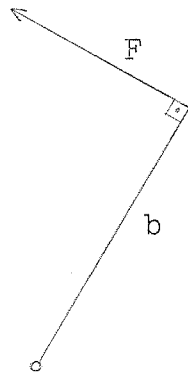


Fig.10 - Torque

In this case the relation gets more complicated by the fact that the force itself depends on the length of the arm. Nevertheless it can be maintained that the torque is proportional

to the length of the arms as is apparent from fig. 9. The proportionality is approximately true for $kb = 5$.

Fig. 11 shows the torque dependency on the length of the arm for constant position angle and phase shift of $\pi/2$. Here again the torque changes from positive to negative values; frequency of these changes as well as magnitude at the peaks of the curve depend on the position angle. As the angle gets smaller, the frequency decreases and the maxima are higher. This is already apparent from figures 7 and 8.

Similarly, plotting torque vs position angle (fig. 12 and 13), we see that torque is 0 at $\phi_0 = \pi$ as is obvious from eq. (35). The number of additional zeros depends on the distance of the antennas from the origin. In fig. 13 curve is drawn to connect the maxima of the individual curves for different kb 's and to make the increase of torque with the distance from the reference point more clear.

It can be expected that additional line sources will increase the torque produced. This would be an advantage only if we satisfy the condition:

$$\frac{T_m}{T_2} > \frac{P_m}{P_2} \quad (38)$$

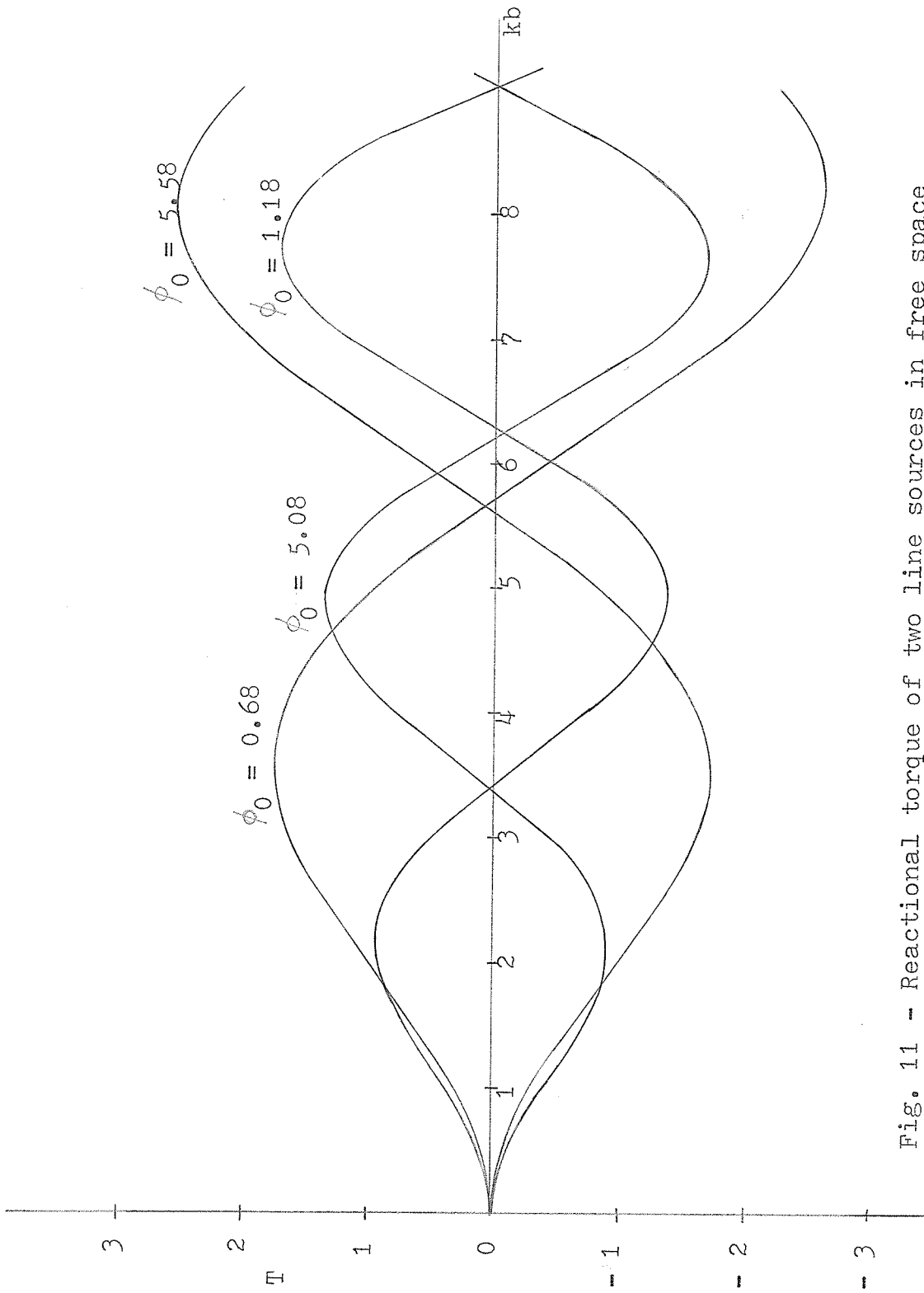


Fig. 11 - Reactional torque of two line sources in free space

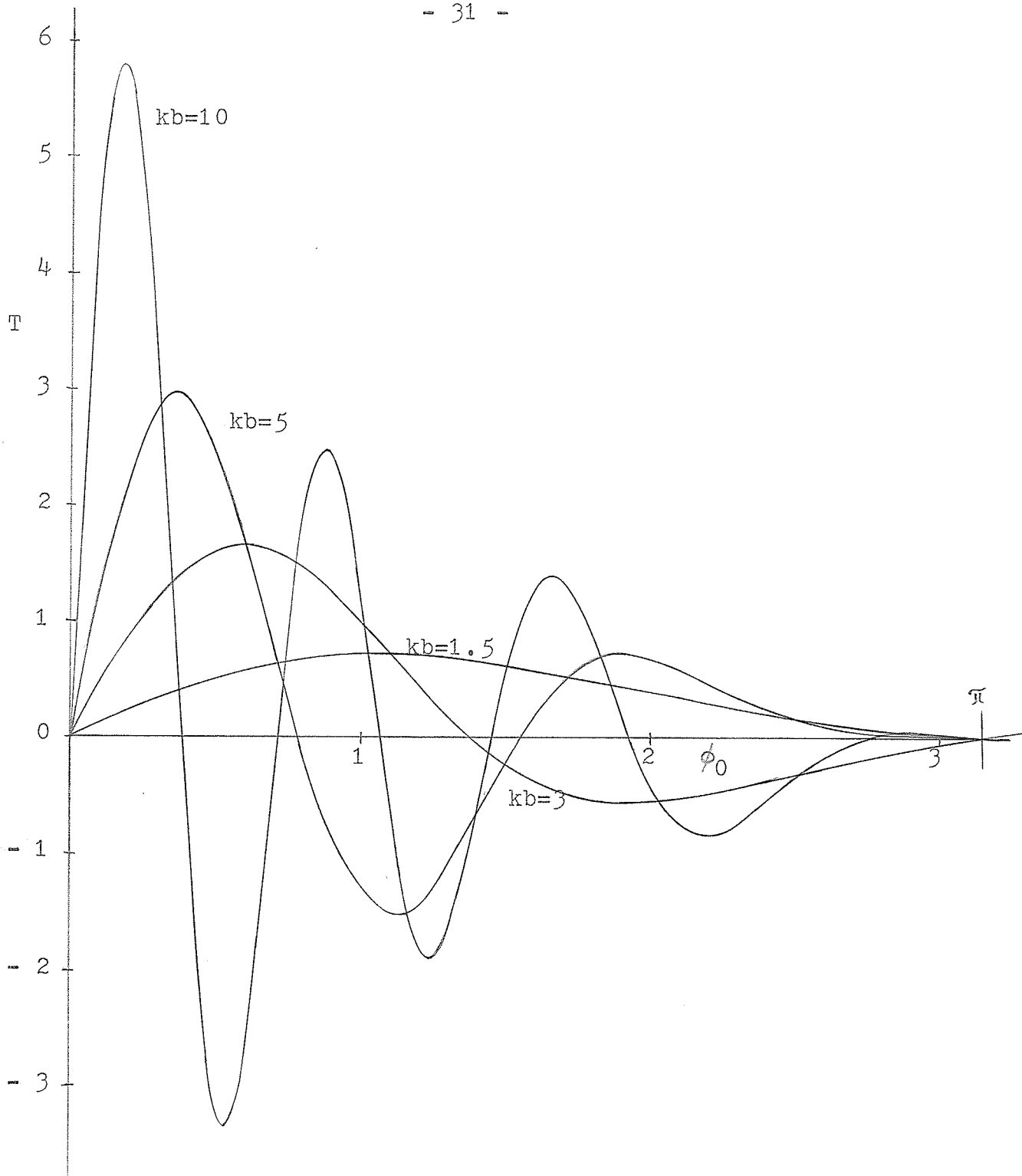


Fig. 12 - Reactional torque of two line sources in free space

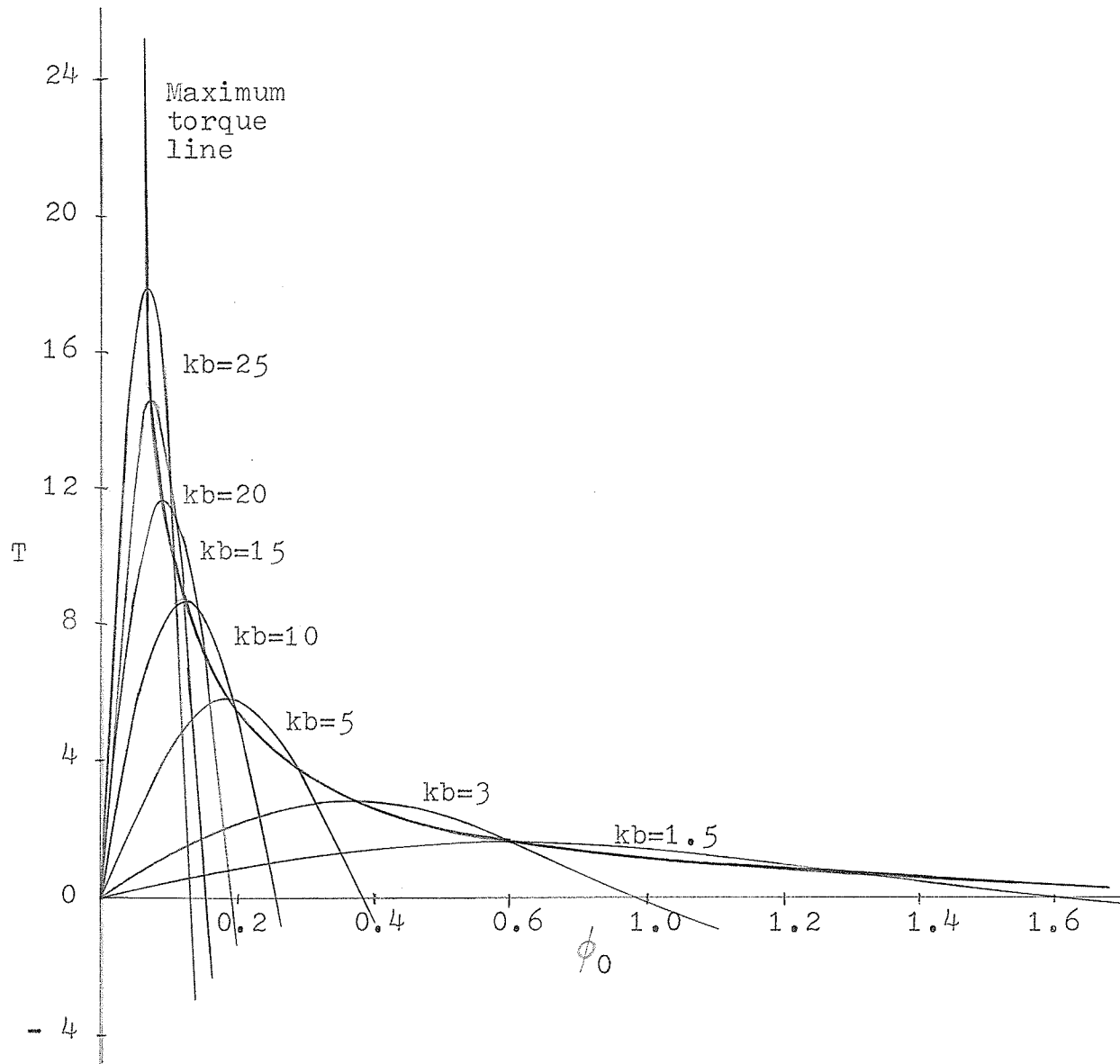


Fig. 13 - Reactional torque of two line sources in free space

In (38) notation T_2 and P_2 for torque and power produced by two sources, and T_m and P_m for torque and power produced by m sources is used.

To what degree it can be achieved is discussed in the coming section III - 3.

III - 3. Line sources equispaced on surface of a cylinder

Consider m line sources that are equispaced on a surface of a circular cylinder. The sources are fixed in their mutual positions, but able to rotate about the axis of the cylinder.

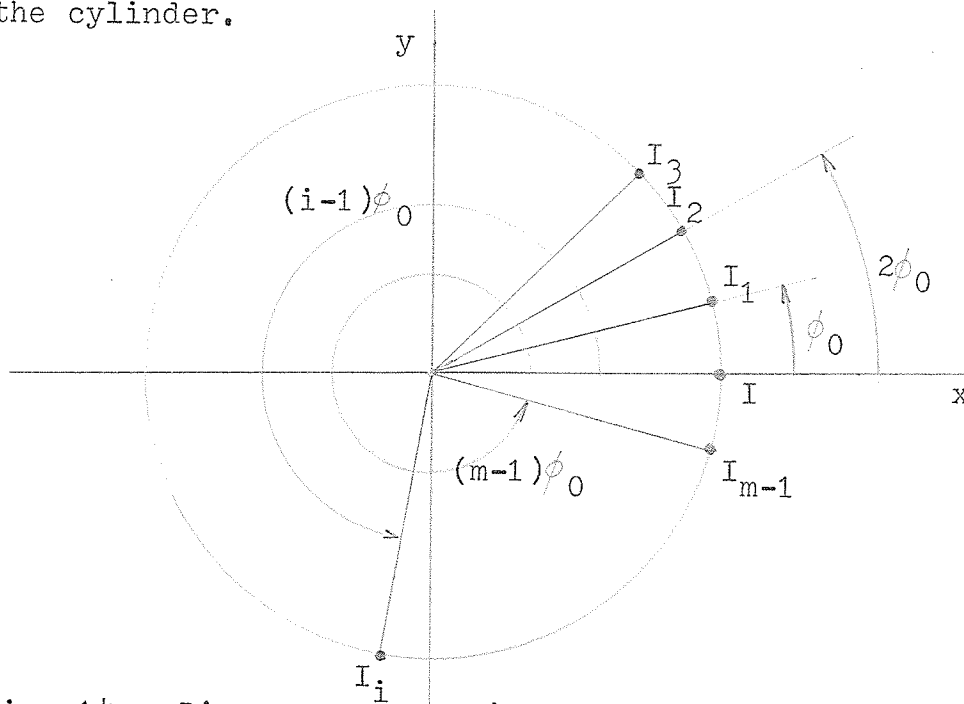


Fig. 14 - Line sources equispaced on surface of a cylinder

Let the currents I_1, \dots, I_{m-1} have an arbitrary phase with respect to I located as shown in fig. 14.

$$I_1 = I \exp(i\gamma_1)$$

$$I_2 = I \exp(i\gamma_2)$$

⋮

$$\begin{matrix} \vdots \\ I_j = I \exp(i\gamma_j) \end{matrix} \quad (39)$$

$$\begin{matrix} \vdots \\ I_{m-1} = I \exp(i\gamma_{m-1}) \end{matrix}$$

Then, by superposition:

$$\psi = \psi_0 + \psi_1 + \psi_2 + \dots + \psi_{m-1} \quad (40)$$

That is, using (19) and (20)

$$\begin{aligned} \psi = \frac{I}{4i} \sum_{n=0}^{\infty} \epsilon_n J_n(kb) H_n^{(2)}(k\rho) \{ \cos n\phi + \exp(i\gamma_1) \cos n(\phi - \phi_0) + \\ + \dots + \exp(i\gamma_{m-1}) \cos [\phi - (m-1)\phi_0] \} \end{aligned}$$

or

$$\psi = \frac{I}{4i} \sum_{n=0}^{\infty} \sum_{p=1}^m \epsilon_n J_n(kb) H_n^{(2)}(k\rho) \exp(i\gamma_{p-1}) \cos[n\phi - (p-1)\phi_0] \quad (41)$$

It follows, since $\frac{\delta}{\delta z} = 0$, that

$$E_\rho = E_\phi = H_z = 0$$

$$E_z = -\frac{k^2 I}{4e_0} \sum_{n=0}^{\infty} \sum_{p=1}^m \epsilon_n J_n(kb) H_n^{(2)}(k\rho) \exp(i\gamma_{p-1}) \cos[n\phi - (p-1)\phi_0] \quad (42)$$

$$H_\phi = - \frac{kI}{4i} \sum_{n=0}^{\infty} \sum_{p=1}^m \epsilon_n J_n(kb) H_n^{(2)}(k\rho) \exp(i\gamma_{p-1}) \cos[n\phi - (p-1)\phi_0] \quad (43)$$

$$H_\rho = - \frac{I}{4i\rho} \sum_{n=0}^{\infty} \sum_{p=1}^m n \epsilon_n J_n(kb) H_n^{(2)}(k\rho) \exp(i\gamma_{p-1}) \sin[n\phi - (p-1)\phi_0] \quad (44)$$

which, similarly as in the case of two line sources, leads to

$$T = \frac{\mu_0}{2} \operatorname{Re} \int_0^{2\pi} \rho^2 H_\rho^* H_\phi d\phi$$

and, after carrying out the integration

$$T = \frac{\mu_0 I^2}{8} \sum_{n=1}^{\infty} \sum_{p=1}^m \sum_{q=1}^m n \epsilon_n [J_n(kb)]^2 \sin n\phi_0 (p-q) \cdot \sin (\gamma_{p-1} - \gamma_{q-1}) \quad (45)$$

For $m = 2$ and $\gamma_1 - \gamma_0 = \pi/2$ eq. (45) reduces to (30b).

The power radiated, using eq. (31) is:

$$P = \frac{\mu_0 I^2}{8} \sum_{n=0}^{\infty} \sum_{p=1}^m \sum_{q=1}^m \epsilon_n [J_n(kb)]^2 \cos n\phi_0 (p-q) \cos (\gamma_{p-1} - \gamma_{q-1}) \quad (46)$$

Once again, for $m = 2$ and $\gamma_1 - \gamma_0 = \pi/2$ we obtain eq. (32).

From equations (45) and (46) it is relatively easy to calculate torque and power for a reasonable number

of current filaments. In the following derivations m is equaled to 3 and later on to 4.

III - 3.1. Three line sources

Substituting $m = 3$ into equations (45) and (46)

we obtain:

$$T_3 = \frac{\mu_0 I^2}{8} \sum_{n=1}^{\infty} \sum_{p=1}^3 \sum_{q=1}^3 n \epsilon_n [J_n(kb)]^2 \sin [n\phi_0(p-q)] \sin (\gamma_{p-1} - \gamma_{q-1}) \quad (47)$$

$$P = \frac{\mu_0 I^2}{8} \sum_{n=0}^{\infty} \sum_{p=1}^3 \sum_{q=1}^3 \epsilon_n [J_n(kb)]^2 \cos n\phi_0(p-q) \cos (\gamma_{p-1} - \gamma_{q-1}) \quad (48)$$

From fig. 15 we have $\phi_0 = 120^\circ$

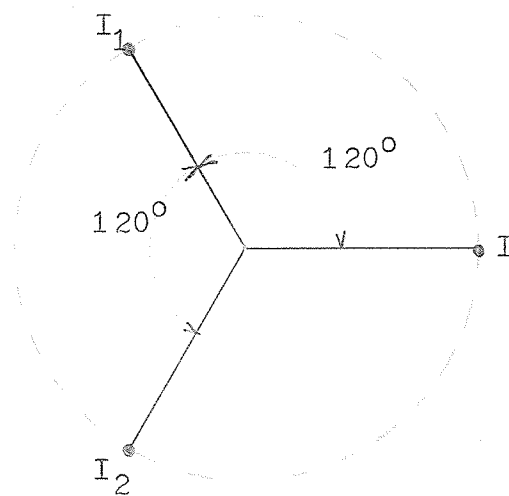


Fig. 15 -

- Configuration of three line sources in free space

By expanding (47) and (48) and adding up the appropriate terms we obtain:

$$T_3 = \frac{\mu_0 I^2}{4} \sum_{n=1}^{\infty} n \epsilon_n [J_n(kb)]^2 \left\{ \sin\left(\frac{2n\pi}{3}\right) \sin(\gamma_1) + \sin(\gamma_2 - \gamma_1) + \right. \\ \left. + \sin\left(\frac{4n\pi}{3}\right) \sin(\gamma_2) \right\} \quad (49)$$

$$P_3 = \frac{\mu_0 I^2 \omega}{8} \sum_{n=0}^{\infty} \epsilon_n [J_n(kb)]^2 \left\{ 3 + 2\cos\left(\frac{2n\pi}{3}\right) [\cos(\gamma_1) + \cos(\gamma_2 - \right. \\ \left. - \gamma_1)] + 2\cos\left(\frac{4n\pi}{3}\right) \cos(\gamma_2) \right\} \quad (50)$$

Let us take a closer look at these two equations. Both of them contain terms which result from the interaction between the individual sources. In eq. (49) the first term is due to the interaction between source 1 and source 2, the second term to 2 and 3 and the third term to 3 and 1. All three of them are consistent with eq. (30a) obtained in Sec. III - 2 for two line sources, if we substitute the corresponding values for γ and ϕ_0 . The expression for power does not come from a simple addition of the individual interactions as is the case in the torque equation. However, here as well, the terms due ^{to} the interactions are clearly separated, and, disregarding the constants, are in agreement with (34).

To help simplify the analysis, assume fixed phases of the three antennas. An obvious choice in this case is:

$$\gamma_1 = 120^\circ$$

$$\gamma_2 = 240^\circ$$

Then

$$T_3 = \frac{3}{2} \mu_0 I^2 \sum_{n=1}^{\infty} n \epsilon_n [J_n(kb)]^2 \sin\left(\frac{2n\pi}{3}\right) \sin^2\left(\frac{n\pi}{3}\right) \quad (51)$$

$$P_3 = \frac{\mu_0 I^2}{4} \sum_{n=1}^{\infty} \epsilon_n [J_n(kb)]^2 \left[2\sin^2\left(\frac{n\pi}{3}\right) + \sin^2\left(\frac{2n\pi}{3}\right) \right] \quad (52)$$

Now

$$\sin^2\left(\frac{n\pi}{3}\right) = \begin{cases} 0 & \text{for } n = 0, 3, 6, 9, \dots \\ \frac{3}{4} & \text{otherwise} \end{cases}$$

and

$$\sin^2\left(\frac{2n\pi}{3}\right) = \begin{cases} 0 & \text{for } n = 0, 3, 6, 9, \dots \\ \frac{3}{4} & \text{otherwise} \end{cases}$$

Therefore we can write

$$\sin^2\left(\frac{n\pi}{3}\right) = \sin^2\left(\frac{2n\pi}{3}\right)$$

and the torque and power equations are:

$$T_3 = 0.5625 \mu_0 I^2 \sum_{\substack{n=1 \\ n \neq 3s}}^{\infty} n \epsilon_n [J_n(kb)]^2 \quad (53)$$

$$P_3 = 0.5625 \mu_0 I^2 \omega \sum_{\substack{n=1 \\ n \neq 3s}}^{\infty} \epsilon_n [J_n(kb)]^2 \quad (54)$$

where $s = 1, 2, 3, \dots$

From (30a) and (33) for two line sources placed $\phi_0 = 120^\circ$ apart we get:

$$T_2 = 0.02165 \mu_0 I^2 \sum_{n=0}^{\infty} n \epsilon_n [J_n(kb)]^2 \frac{2}{3} \sin\left(\frac{2n\pi}{3}\right) \quad (55)$$

in which

$$\frac{2}{3} \sin\left(\frac{2n\pi}{3}\right) = \begin{cases} +1 & \text{for } n = 1, 4, 7, 10, \dots \\ -1 & \text{for } n = 2, 5, 8, 11, \dots \\ 0 & \text{for } n = 0, 3, 6, 9, \dots \end{cases}$$

(This form has been chosen for an easier comparison with (53))

The power in this case is:

$$P_2 = 0.25 \mu_0 I^2 \omega \quad (56)$$

We can now see that

$$P_3 = 2.25 P_2 \sum_{\substack{n=0 \\ n \neq 3s}}^{\infty} \epsilon_n [J_n(kb)]^2 \quad (57)$$

In view of

$$\sum_{n=0}^{\infty} \epsilon_n [J_n(kb)]^2 = 1$$

we can assess that

$$\sum_{\substack{n=0 \\ n \neq 3s}}^{\infty} \epsilon_n [J_n(kb)]^2 < 1$$

and therefore

$$P_3 < 2.25 P_2 \quad (58)$$

Similarly

$$T_3 > 2.6 T_2 \quad (59)$$

This makes the gain in torque at least 1.15 times greater than the gain in power.

Fig. (17) shows the relative values of $\frac{T_3}{P_3}$, $\frac{T_2}{P_2}$ and $\frac{T_2^{\max}}{P_2}$ versus the length of the arm. (T_2^{\max} is the

maximum torque for the fixed value of kb . The angle ϕ_0 is not necessarily a constant in this case). It is apparent, that torque/power ratio can be more significantly improved by an addition of a third antenna than by rearranging the two antenna configuration, although this improvement is very slight for some values of kb .

The above discussed results lead us to an opinion that an additional antenna will further improve the torque efficiency.

III - 3.2. Four line sources

If $m = 4$, following the same procedure,

$$T_4 = \frac{\mu_0 I^2}{8} \sum_{n=1}^{\infty} \sum_{p=1}^4 \sum_{q=1}^4 \epsilon_n [J_n(kb)]^2 \sin n\phi_0(p - q) \cdot \sin(\gamma_{p-1} - \gamma_{q-1}) \quad (60)$$

$$P_4 = \frac{\mu_0 I^2 \omega}{8} \sum_{n=0}^{\infty} \sum_{p=1}^4 \sum_{q=1}^4 \epsilon_n [J_n(kb)]^2 \cos n\phi_0(p - q) \cdot \cos(\gamma_{p-1} - \gamma_{q-1}) \quad (61)$$

From fig. 16 it is apparent that this time $\phi_0 = \pi/2$

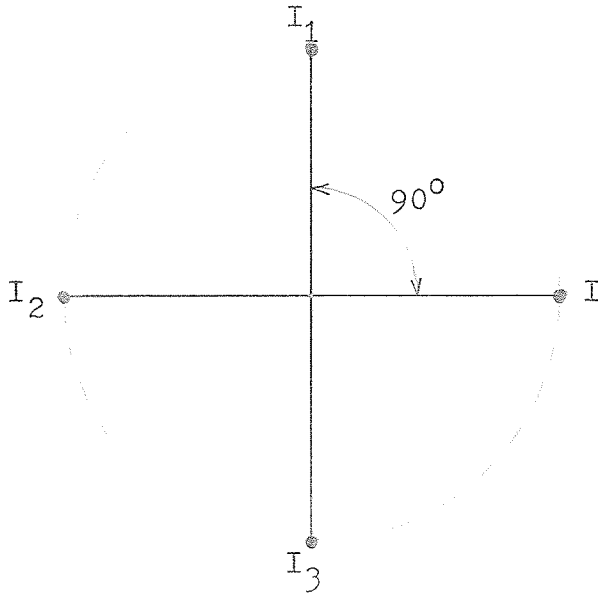


Fig. 16

After the expansion and a little manipulation

$$T_4 = \frac{\mu_0 I^2}{4} \sum_{n=1}^{\infty} n \epsilon_n [J_n(kb)]^2 \sin\left(\frac{n\pi}{2}\right) \left\{ [\sin\gamma_1 + \sin\gamma_2 + \right. \\ \left. + \sin(\gamma_3 - \gamma_2)] + \sin\left(\frac{3n\pi}{2}\right) \sin\gamma_3 \right\} \quad (62)$$

$$P_4 = \frac{\mu_0 I^2 \omega}{4} \sum_{n=0}^{\infty} \epsilon_n [J_n(kb)]^2 \left\{ 2 + \cos\left(\frac{n\pi}{2}\right) [\cos\gamma_1 + \cos\gamma_2 + \right. \\ \left. + \cos(\gamma_3 - \gamma_2)] + \cos(n\pi) [\cos\gamma_2 + \cos(\gamma_3 - \gamma_1)] + \right. \\ \left. + \cos\left(\frac{3n\pi}{2}\right) \cos\gamma_3 \right\} \quad (63)$$

If we want to keep the phase constant, we may choose:

$$\begin{aligned} \gamma_1 &= \pi/2 \\ \gamma_2 &= \pi \\ \gamma_3 &= 3\pi/2 \end{aligned}$$

It reduces (62) and (63) to:

$$T_4 = \mu_0 I^2 \sum_{n=1}^{\infty} n \epsilon_n [J_n(kb)]^2 \sin^3\left(\frac{n\pi}{2}\right) \quad (64)$$

$$P_4 = \mu_0 I^2 \omega \sum_{n=0}^{\infty} \epsilon_n [J_n(kb)]^2 [1 - (-1)^n] \quad (65)$$

In eq. (64) $\sin\left(\frac{n\pi}{2}\right)$ takes on 0 and ± 1 values. Evidently $\sin^3\left(\frac{n\pi}{2}\right) = \sin\left(\frac{n\pi}{2}\right)$. Then

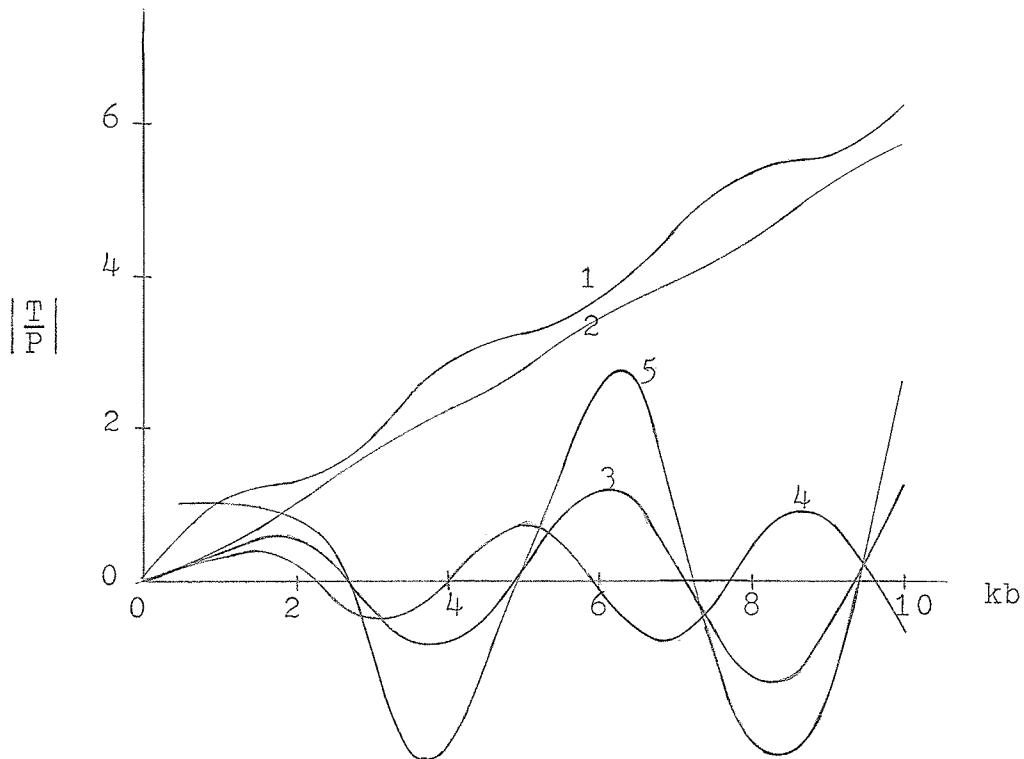
$$T_4 = \mu_0 I^2 \sum_{n=1}^{\infty} n \epsilon_n [J_n(kb)]^2 \sin\left(\frac{n\pi}{2}\right) \quad (66)$$

This form makes it easy to compare it with the relationship obtained in Sec. III - 2, eq. (30b) for two line sources, placed $\phi_0 = \pi/2$ apart:

$$T_2 = \frac{\mu_0 I^2}{4} \sum_{n=1}^{\infty} n \epsilon_n [J_n(kb)]^2 \sin\left(\frac{n\pi}{2}\right) \quad (67)$$

Clearly

$$T_4 = 4 T_2 \quad (68)$$



- 1 - three line sources, $\gamma = 120^\circ$, $\phi_0 = 120^\circ$
- 2 - two line sources, the maximum T/P ratio for given kb
- 3 - two line sources, $\gamma = 90^\circ$, $\phi_0 = 90^\circ$
- 4 - two line sources, $\gamma = 90^\circ$, $\phi_0 = 120^\circ$
- 5 - four line sources, $\gamma = 90^\circ$, $\phi_0 = 90^\circ$

Fig. 17 - Torque/power ratio of two, three and four sources configurations in free space

As to the power relations:

$$P_2 = \frac{\mu_0 I^2 \omega}{4} \sum_{n=0}^{\infty} \epsilon_n [J_n(kb)]^2$$

$$P_4 = \frac{\mu_0 I^2 \omega}{2} \sum_{n=0}^{\infty} \epsilon_n [J_n(kb)]^2 [1 - (-1)^n] < 4P_2$$

It can be safely stated that the gain in torque surpasses the gain in power and thus makes this arrangement more efficient than the 2 line sources. However, from fig.(17) the comparison with the 3 line sources arrangement reveals that torque efficiency decreases for the values of kb greater than 0.9.

For a general case the torque and power relations given by (45) and (46) are in too complicated a form to be discussed here. It would be necessary to reduce the equations for each specific case of given m as was done for m = 3 and m = 4. It can be reasonably expected from what was just shown that for some of m > 4 the torque will increase more rapidly than the power, thus making these line sources arrangements more desirable than 2 line sources ones.

In the following section the line sources are placed close to a cylinder. We are going to consider the two line sources configurations only. For m > 2 the calculations would follow the same steps, with the only difference of using equations (42) through (44) as an incident field.

IV. LINE SOURCES AT THE PRESENCE OF A CYLINDER

In practice antennas are usually supported by a construction. To account for the effect of such an obstacle two cases are considered in this chapter: two line sources close to a conducting cylinder, and, in the second section, two line sources close to a dielectric cylinder.

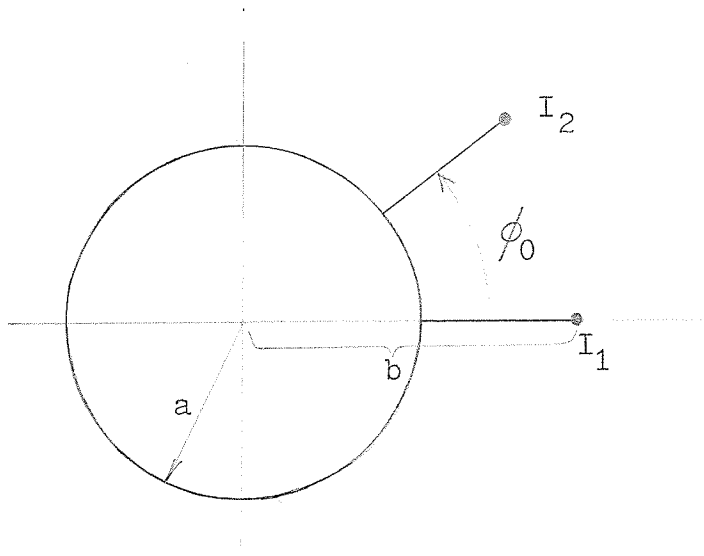


Fig. 18 - Arrangement of two line sources close to a conducting cylinder

IV - 1. Line sources and an infinite conducting cylinder.

As in Sec. III - 2 the same presuppositions are imposed on the line sources and the supporting arms. The cylinder itself is assumed to be conducting with an infinite conductivity. The currents are uniformly distributed along the lines. Their phase difference is .

$$I_1 = I$$

$$I_2 = I \exp(i\gamma)$$

The incident wave function and fields are given by equations (24) through (27). The total wave function is the sum of the incident and scattered wave functions; the scattered wave function itself has the form:

$$\psi_{sc} = \frac{I}{4i} \sum_{n=-\infty}^{\infty} A_n H_n^{(2)}(kb) H_n^{(2)}(k\rho) \exp(in\phi) [1 + \exp(i\gamma - in\phi_0)] \quad (69)$$

Then

$$\begin{aligned} \psi_{total} &= \psi_{inc} + \psi_{sc} = \\ &= \frac{I}{4i} \sum_{n=-\infty}^{\infty} [J_n(k\rho) + A_n H_n^{(2)}(k\rho)] H_n^{(2)}(kb) \exp(in\phi) \cdot \\ &\quad \cdot [1 + \exp(i\gamma - in\phi_0)] \quad \rho < b \end{aligned}$$

$$\begin{aligned} \psi_{total} &= \frac{I}{4i} \sum_{n=-\infty}^{\infty} [J_n(kb) + A_n H_n^{(2)}(kb)] H_n^{(2)}(k\rho) \exp(in\phi) \cdot \\ &\cdot [1 + \exp(i\gamma - in\phi_0)] \quad \rho > b \end{aligned} \quad (70)$$

Constant A_n is found from the boundary conditions on the cylinder and is equal to:

$$A_n = - \frac{J_n(ka)}{H_n^{(2)}(ka)} \quad (71)$$

The electromagnetic field outside of the cylinder for $\rho > b$ is:

$$E_\rho = E_\phi = H_z = 0$$

$$\begin{aligned} E_z &= - \frac{k^2 I}{4\epsilon_0 \omega} \sum_{n=-\infty}^{\infty} [J_n(kb) + A_n H_n^{(2)}(kb)] H_n^{(2)}(k\rho) \exp(in\phi) \cdot \\ &\cdot [1 + \exp(i\gamma - in\phi_0)] \end{aligned} \quad (72)$$

$$\begin{aligned} H_\rho &= \frac{I}{4\rho} \sum_{n=-\infty}^{\infty} n [J_n(kb) + A_n H_n^{(2)}(kb)] H_n^{(2)}(k\rho) \exp(in\phi) \cdot \\ &\cdot [1 + \exp(i\gamma - in\phi_0)] \end{aligned} \quad (73)$$

$$\begin{aligned} H_\phi &= - \frac{kI}{4i} \sum_{n=-\infty}^{\infty} [J_n(kb) + A_n H_n^{(2)}(kb)] H_n^{(2)}(k\rho) \exp(in\phi) \cdot \\ &\cdot [1 + \exp(i\gamma - in\phi_0)] \end{aligned} \quad (74)$$

By a similar procedure as in Sec. III - 2 and using equations (17) and (31), the torque and the power are obtained:

$$T = \frac{\mu_0 I^2}{4} \sin(\gamma) \sum_{n=0}^{\infty} \epsilon_n n \sin(n\phi_0) K_n K_n^* \quad (75)$$

$$P = \frac{\mu_0 I^2 \omega}{4} \sum_{n=0}^{\infty} \epsilon_n [1 + \cos(n\phi_0) \cos(\gamma)] K_n K_n^* \quad (76)$$

where

$$K_n = J_n(kb) - \frac{J_n(ka)}{H_n^{(2)}(ka)} H_n^{(2)}(kb) \quad (77)$$

In the case $\gamma = \pi/2$

$$T = \frac{\mu_0 I^2}{4} \sum_{n=0}^{\infty} \epsilon_n n \sin(n\phi_0) K_n K_n^* \quad (78)$$

$$P = \frac{\mu_0 I^2 \omega}{4} \sum_{n=0}^{\infty} \epsilon_n K_n K_n^* \quad (79)$$

so that

$$M = \omega \frac{T}{P} = \frac{\sum_{n=0}^{\infty} \epsilon_n n \sin(n\phi_0) K_n K_n^*}{\sum_{n=0}^{\infty} \epsilon_n K_n K_n^*} \quad (80)$$

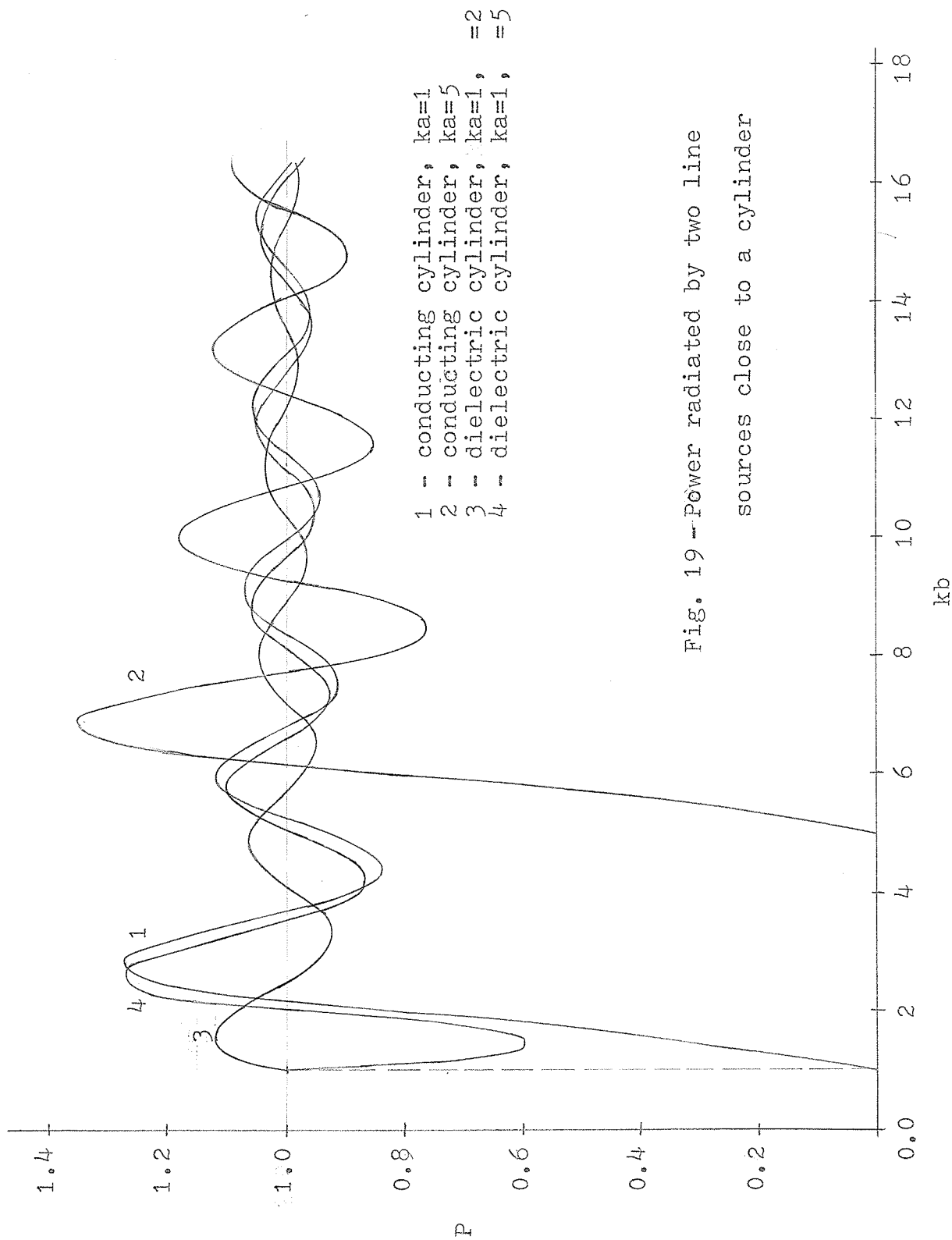
The power radiated is given by eq. (79). Comparing it with eq. (34b) we see that the term in the front of the summation is actually power radiated by the two line sources

in a free space. Since the phase difference is $\gamma = \pi/2$, there is no modification of power due to the influence of one source on the other one and the summation term

$$\sum_{n=0}^{\infty} \epsilon_n K_n K_n^*$$

can be fully attributed to the presence of the cylinder. The relative value of the power vs the distance of the antenna from the reference point is plotted in fig. (19). As the cylinder diameter increases, the maximum power attains higher values. The maximum lies at about $(kb - ka) = 1.9$. If the distance of the line sources from the cylinder gets very large, the influence of the cylinder becomes negligible.

By placing the sources close to a conducting cylinder the torque/power ratio is affected only slightly, as can be seen from the comparison of fig. (8) and fig.'s (20) through (23). The maximum ratio is again at about $d/\lambda = 0.29$. If the antennas are placed very close to the cylinder ($(kb - ka) = 2$), the most apparent difference is a shift of the first zero of the curve towards a larger relative distance as in fig. (23) for $ka = 8$ and $kb = 10$ or in fig. (22) for $ka = 4$ and $kb = 5$. The deviations in the maximum torque for some kb 's and ka 's are shown in fig. (9). There is no obvious pattern in the changes, except that the deviations (in both



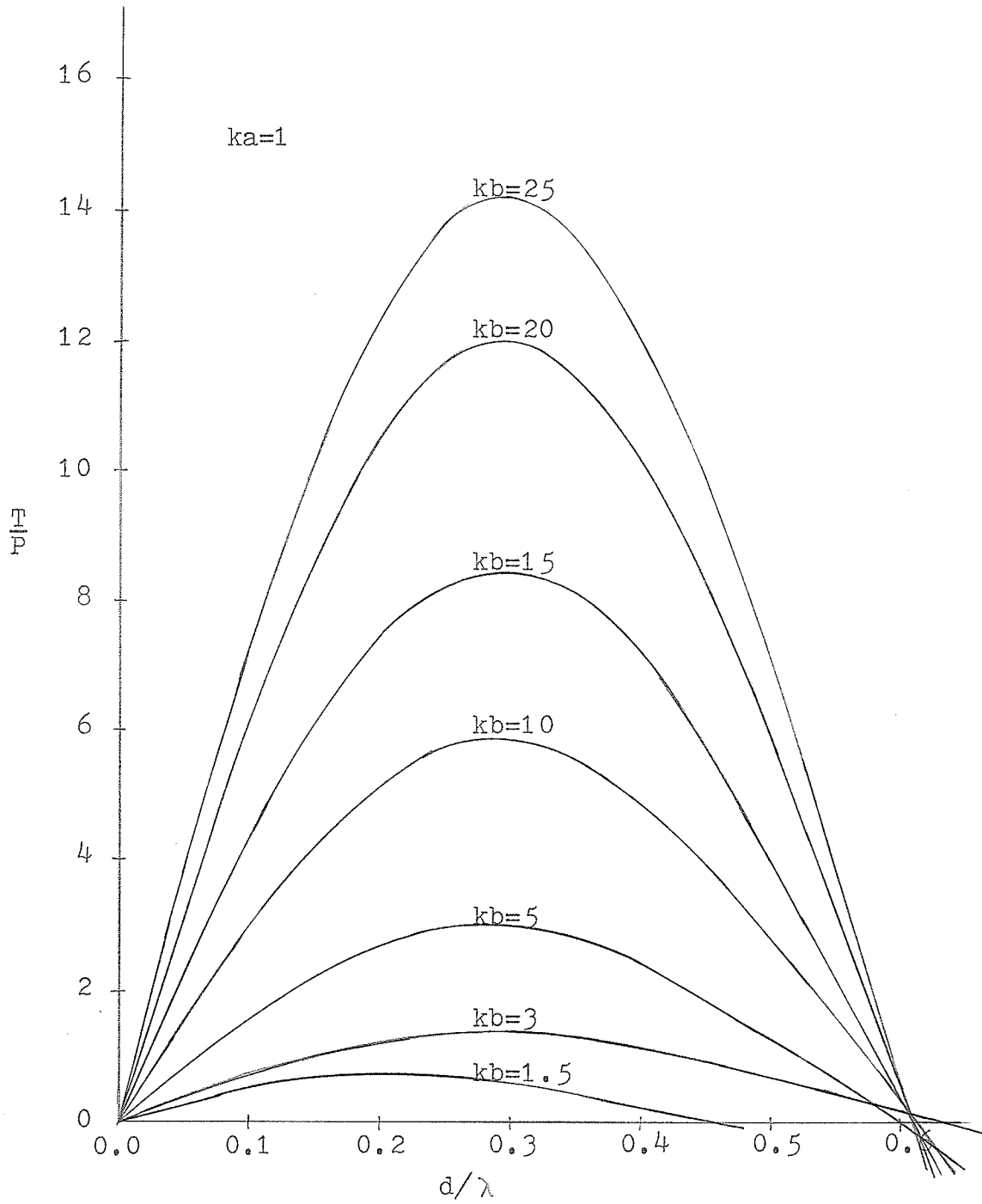


Fig. 20 - Torque/power ratio of two line sources close to a conducting cylinder.

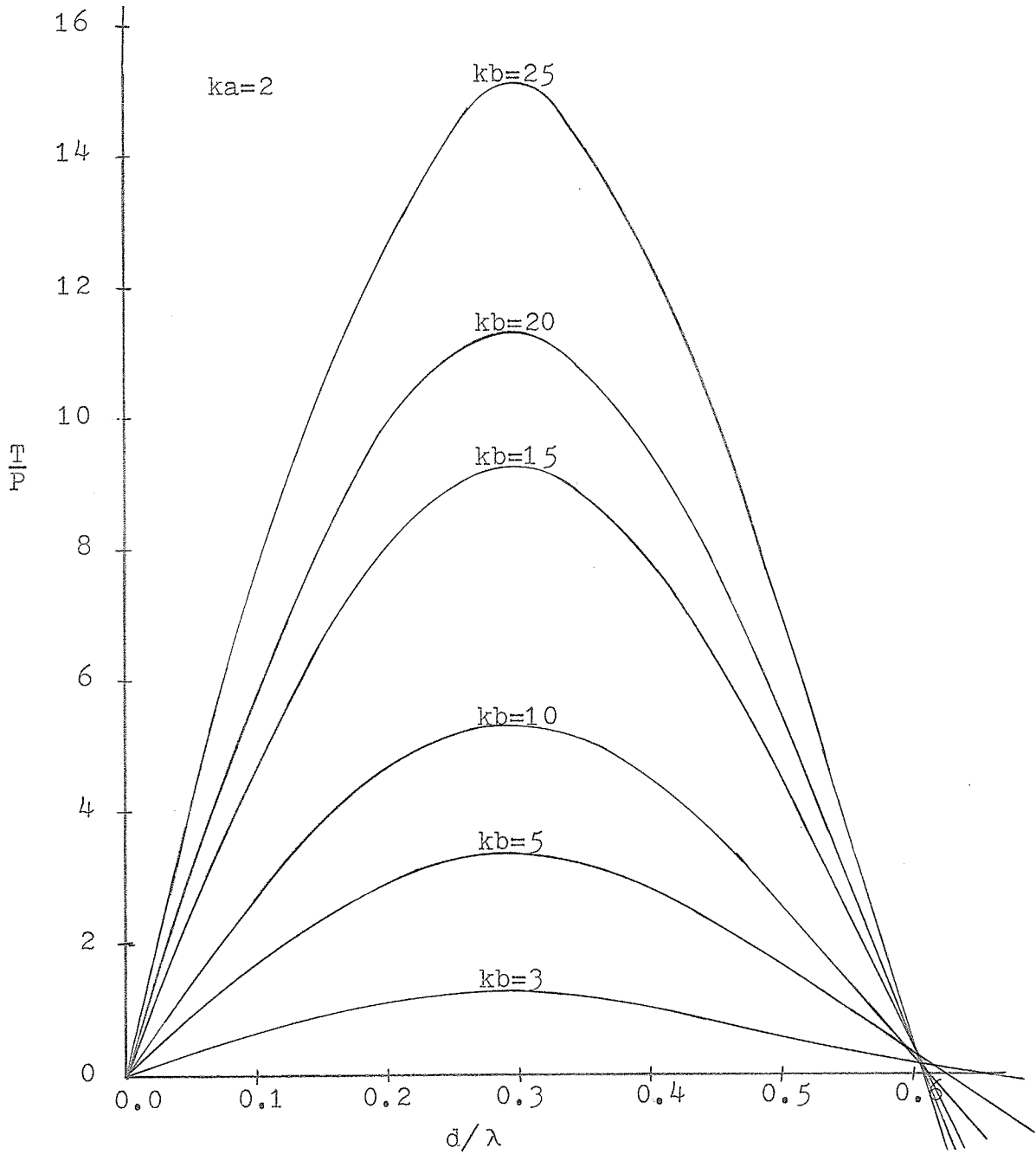


Fig. 21 - Torque/power ratio of two line sources close to a conducting cylinder

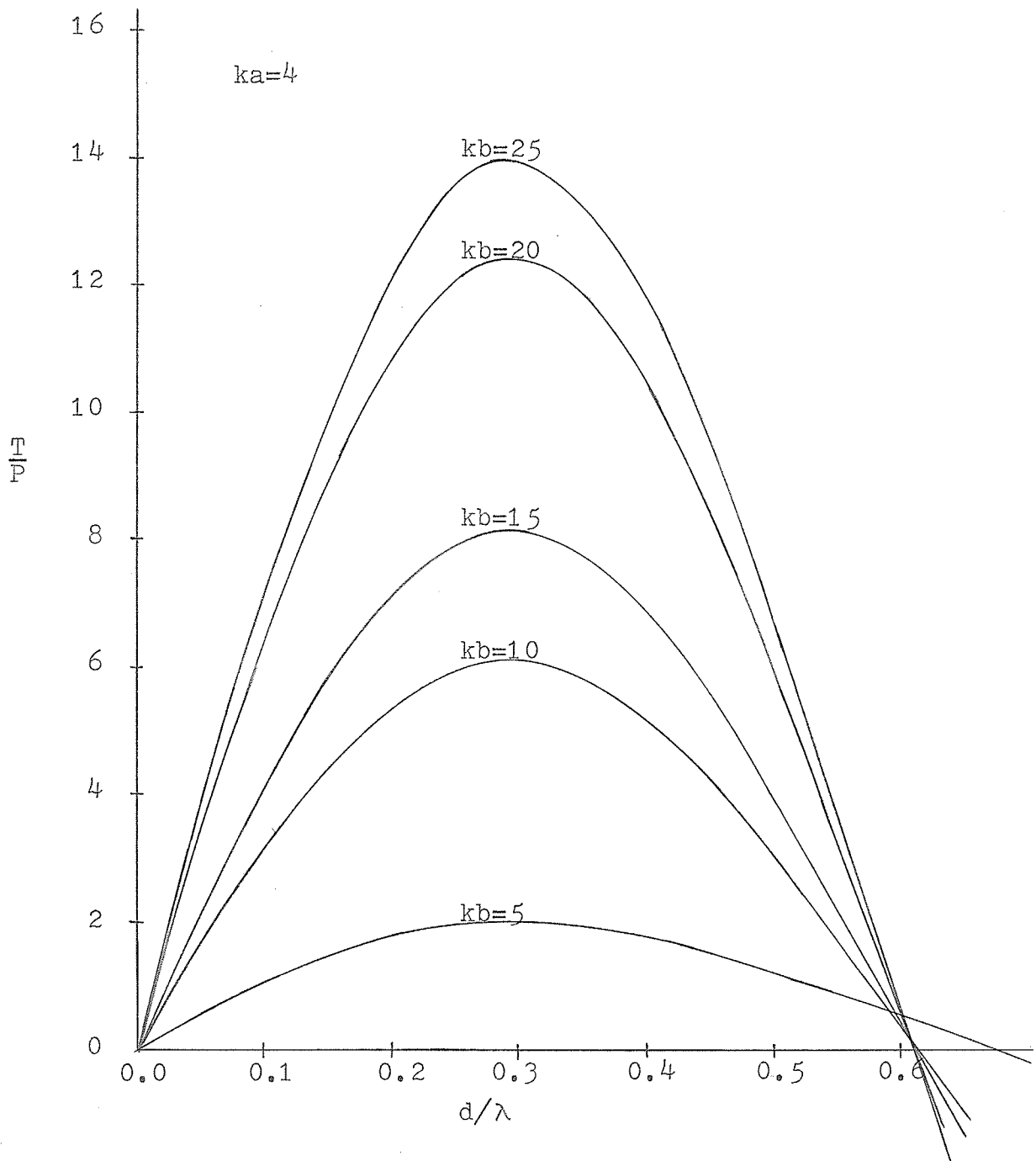


Fig. 22 - Torque/power ratio of two line sources close to a conducting cylinder

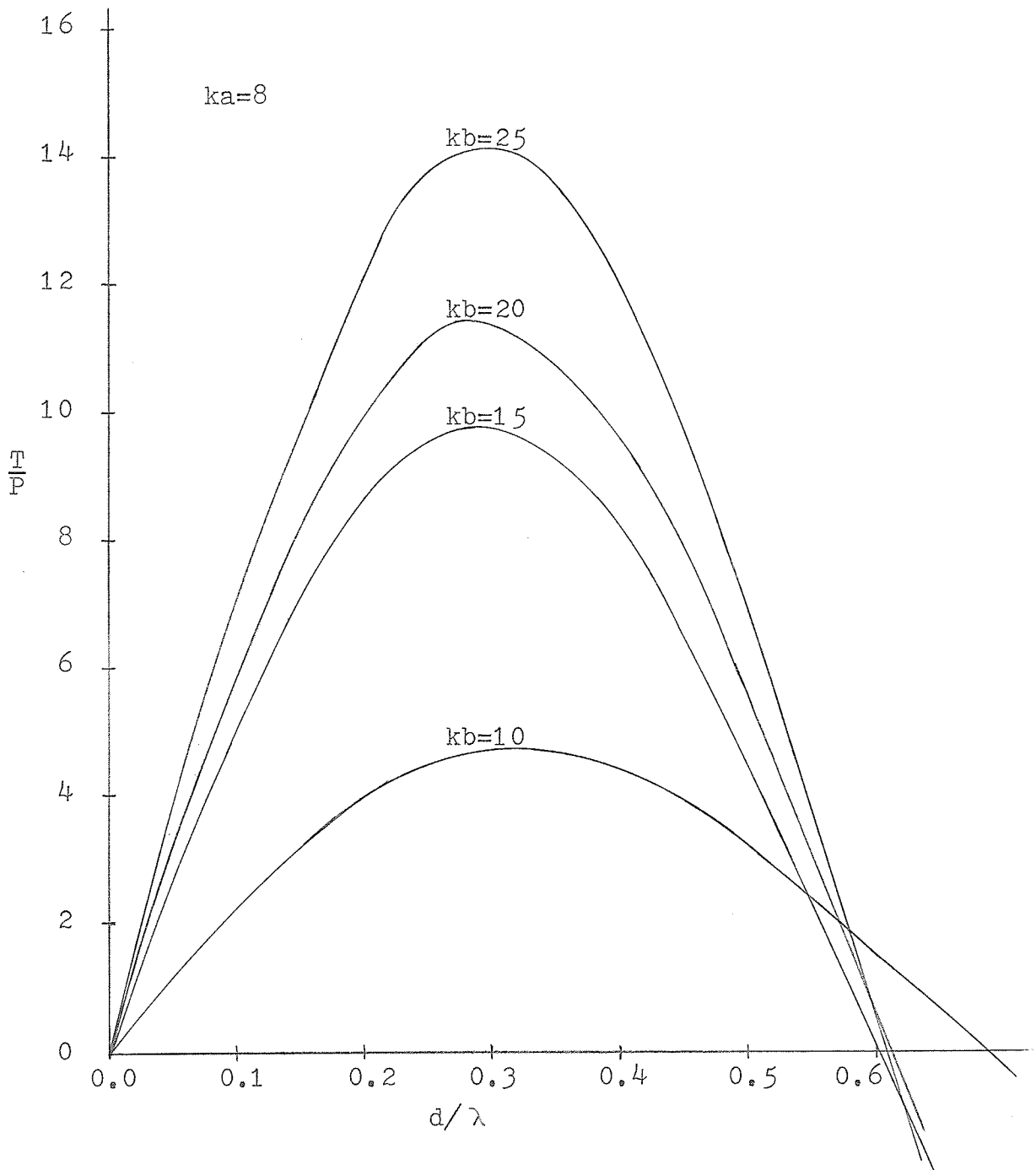


Fig. 23 - Torque/power ratio of two line sources close to a conducting cylinder

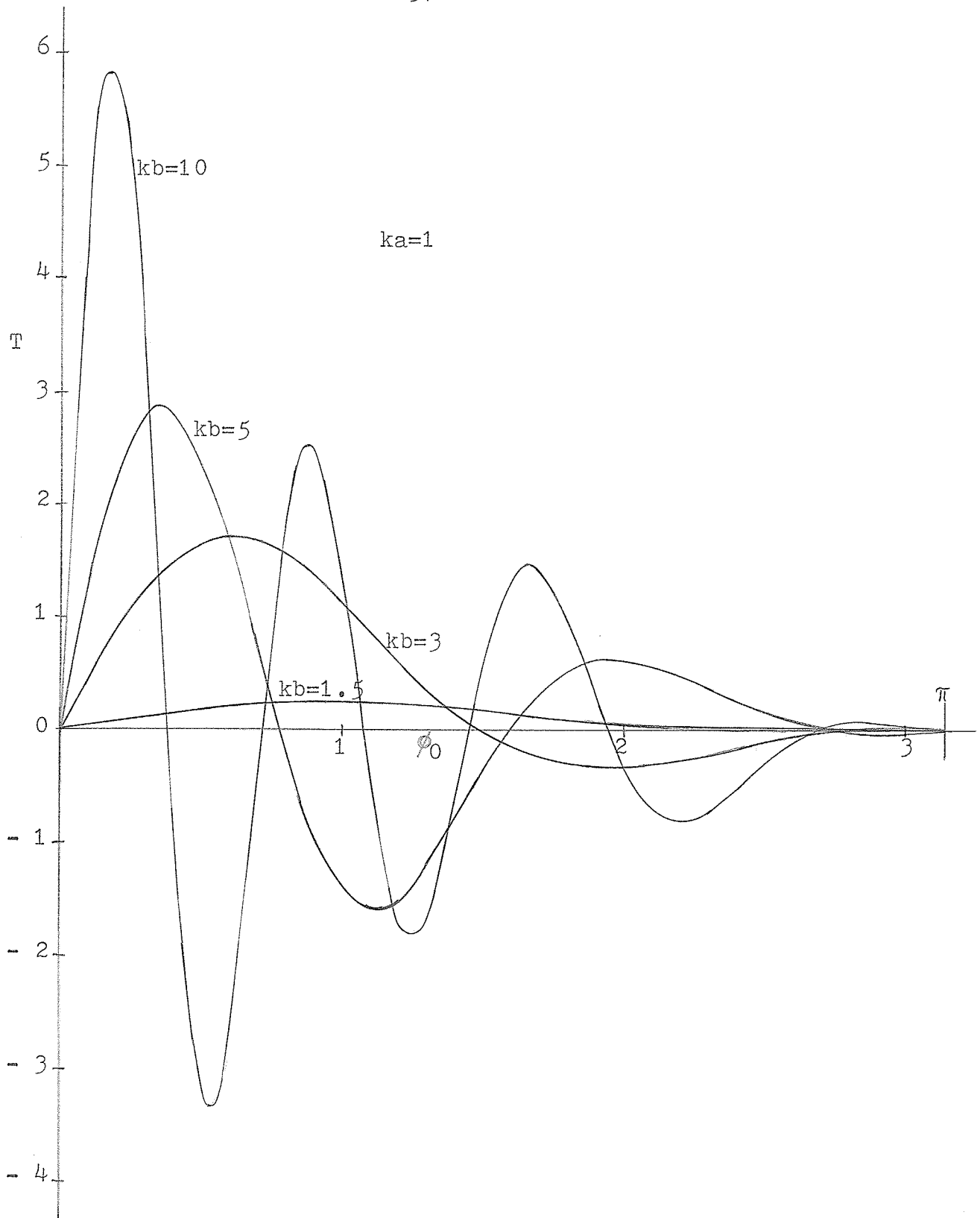


Fig. 24 - Reactional torque of two line sources close to a conducting cylinder

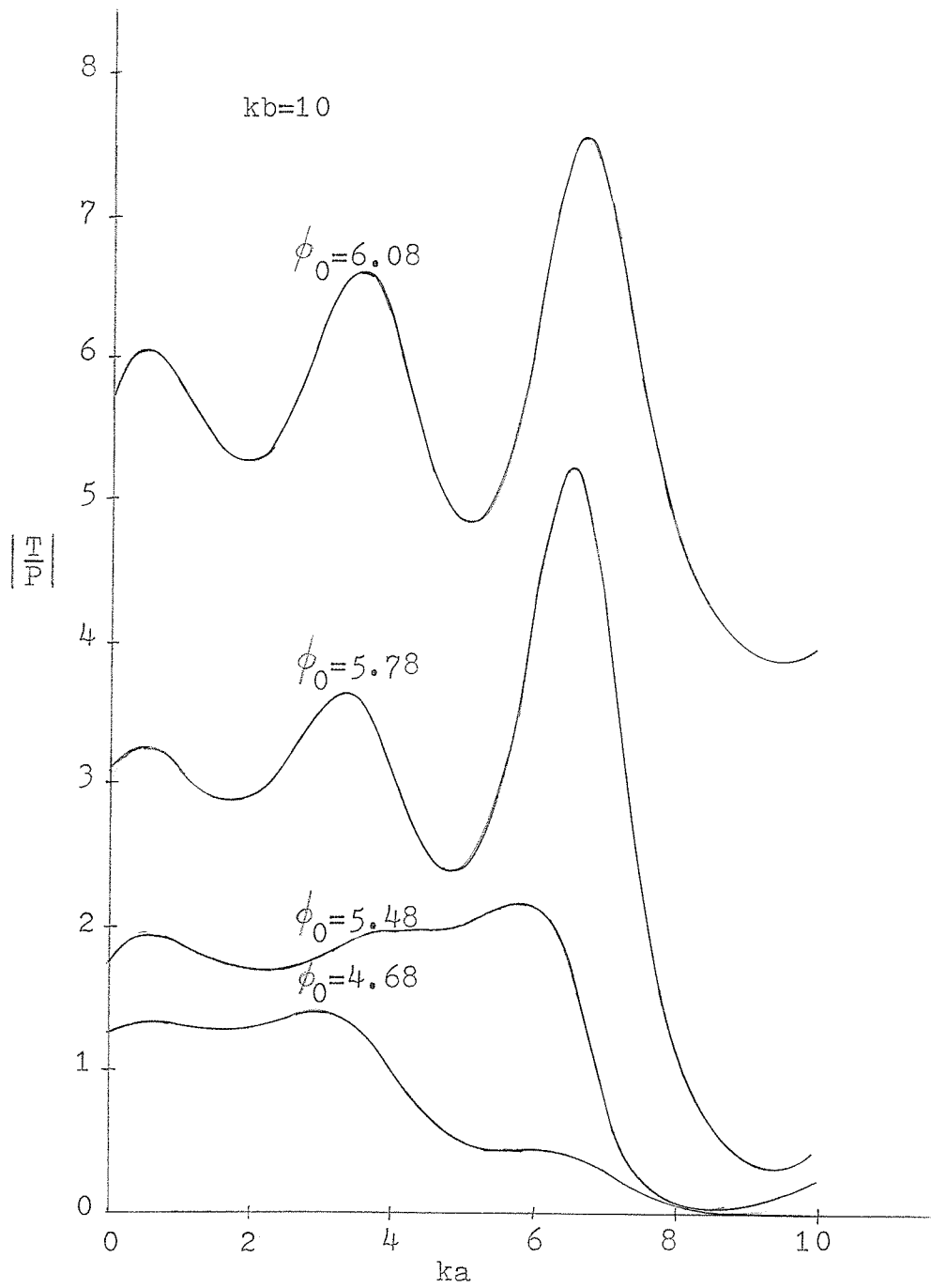


Fig. 25 - Torque/power ratio of the line sources close to a conducting cylinder; cylinder radius is the independent variable

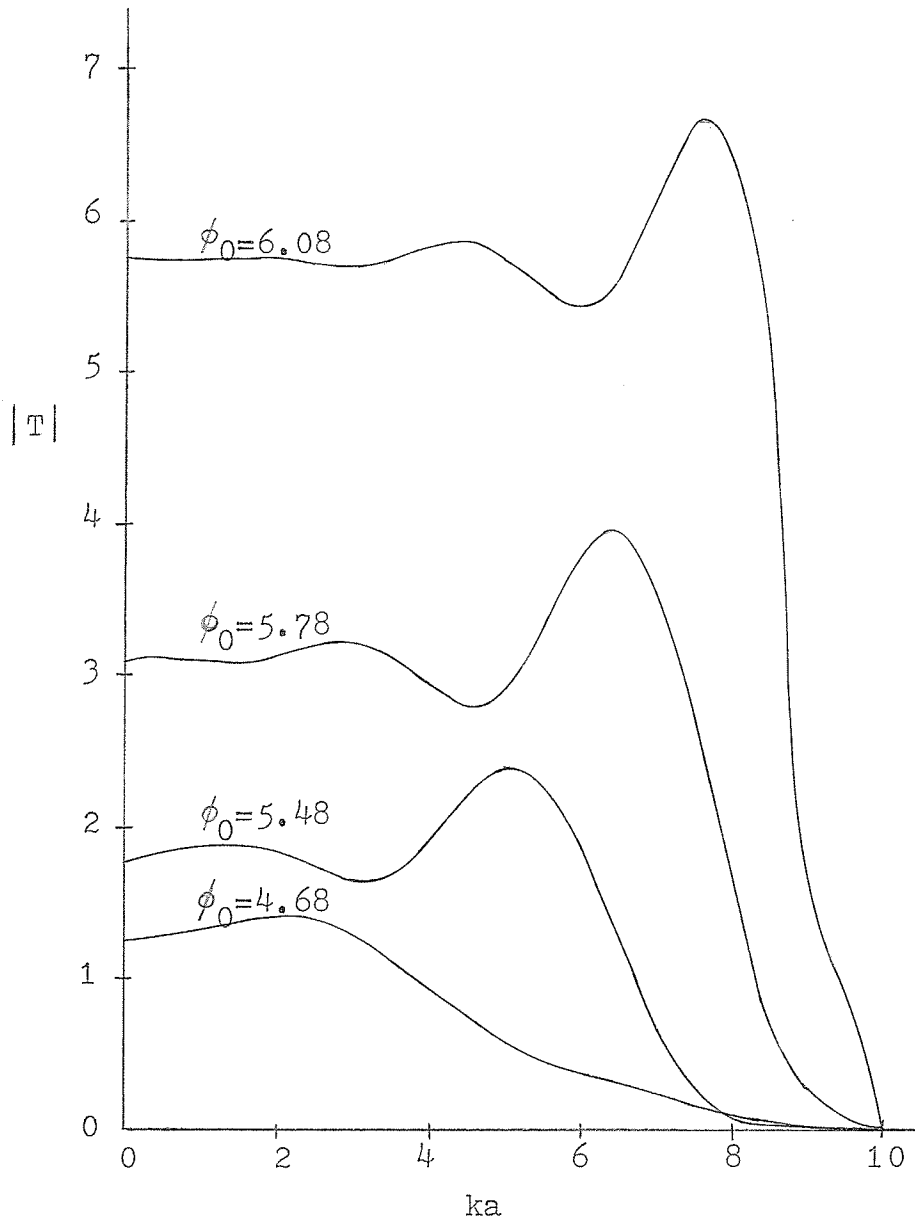


Fig. 26 - Torque of two line sources close to a conducting cylinder; cylinder radius is the independent variable

directions) tend to get larger for larger cylinders.

The curves showing the dependency of the torque on the mutual position angle ϕ_0 of the antennas are in fig. (24). There is no substantial change from the case of the line sources without any cylinder nearby..

If the distance of the sources from origin is kept constant and the radius of the cylinder is gradually increased from 0 to b , sets of curves of fig.'s (25) and (26) are obtained. At $a = b$ both power and torque are equal 0. Maximum torque (as well as the maximum torque/power ratio) is higher if the sources are placed closer together. However, to achieve the maximum, a cylinder of larger radius is then required.

It has been shown that a supporting construction which can be approximated by a conducting cylinder does not significantly influence the torque/power ratio. The situation may be different if dielectric materials for the supports are used. To account for this possibility a dielectric cylinder, instead of the conducting one, is introduced into the configuration in the following section IV - 2.

IV - 2. Line sources and an infinite dielectric cylinder.

Suitable dielectric materials often enhance power efficiency of antennas. Although the configuration that is investigated is somewhat different from the usually presented problems, we can expect the effect on the torque/power ratio be more pronounced than it was in the conducting cylinder case.

The configuration is identical as in the previous section in the case of the conducting cylinder. The permittivity of the dielectric cylinder is ϵ_d , the wave number is k_d . We assume the permeability to be that of the free space μ_0 .

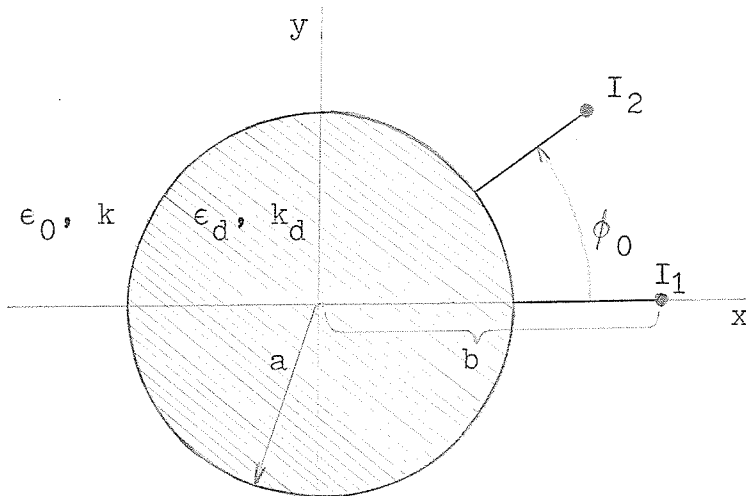


Fig. 27 - Arrangement of two line sources close to a dielectric cylinder

The current distributions along the line sources are:

$$I_1 = I$$

$$I_2 = I \exp(i\gamma)$$

The incident and scattered wave functions are given by:

$$\psi_{\text{inc}} = \begin{cases} \frac{I}{4i} \sum_{n=-\infty}^{\infty} H_n^{(2)}(kb) J_n(k\rho) \exp(in\phi) [1 + \exp(i\gamma - in\phi_0)] & \rho < b \\ \frac{I}{4i} \sum_{n=-\infty}^{\infty} J_n(kb) H_n^{(2)}(k\rho) \exp(in\phi) [1 + \exp(i\gamma - in\phi_0)] & \rho > b \end{cases} \quad (81)$$

$$\psi_{\text{sc}} = \frac{I}{4i} \sum_{n=-\infty}^{\infty} C_n H_n^{(2)}(k\rho) \exp(in\phi) [1 + \exp(i\gamma - in\phi_0)] \quad (82)$$

The transmitted wave function inside of the cylinder:

$$\psi_{\text{tr}} = \frac{I}{4i} \sum_{n=-\infty}^{\infty} D_n J_n(k_d b) \exp(in\phi) [1 + \exp(i\gamma - in\phi_0)] \quad (83)$$

From the boundary conditions at $\rho = a$

$$H_{\phi, \text{tr}} = H_{\phi, \text{inc}} + H_{\phi, \text{sc}}$$

$$E_{z, \text{tr}} = E_{z, \text{inc}} + E_{z, \text{sc}}$$

the constants C_n and D_n are:

$$C_n = H_n^{(2)}(kb) \frac{\epsilon_0 k_d J_n'(ka) J_n(k_d a) - k \epsilon_d J_n(ka) J_n'(k_d a)}{\epsilon_d k H_n^{(2)}(ka) J_n'(k_d a) - k \epsilon_0 J_n(k_d a) H_n^{(2)}(ka)} \quad (84)$$

$$D_n = \frac{k^2 \epsilon_d}{k_d} H_n^{(2)}(kb) \frac{J_n'(ka) H_n^{(2)}(ka) - J_n(ka) H_n'^{(2)}(ka)}{\epsilon_d k H_n^{(2)}(ka) J_n'(k_d a) - k \epsilon_0 J_n(k_d a) H_n'^{(2)}(ka)} \quad (85)$$

The electric and magnetic fields outside of the cylinder for $\rho > b$ are:

$$E_\rho = E_\phi = H_z = 0$$

$$E_z = - \frac{k^2 I}{4 \epsilon_0 \omega} \sum_{n=-\infty}^{\infty} H_n^{(2)}(k\rho) [J_n(kb) + C_n] \exp(in\phi) [1 + \exp(i\gamma - in\phi_0)] \quad (86)$$

$$H_\rho = - \frac{I}{4i\rho} \sum_{n=-\infty}^{\infty} n H_n^{(2)}(k\rho) [J_n(kb) + C_n] \exp(in\phi) [1 + \exp(i\gamma - in\phi_0)] \quad (87)$$

$$H_\phi = - \frac{kI}{4i} \sum_{n=-\infty}^{\infty} H_n'^{(2)}(k\rho) [J_n(kb) + C_n] \exp(in\phi) [1 + \exp(i\gamma - in\phi_0)] \quad (88)$$

It follows that:

$$T = \frac{\mu_0 I^2}{4} \sin(\gamma) \sum_{n=0}^{\infty} n \epsilon_n \sin(n\phi_0) [J_n(kb) + C_n]^2 \quad (89)$$

$$P = \frac{\mu_0 I^2 \omega}{4} \sum_{n=0}^{\infty} \epsilon_n [1 + \cos(n\phi_0) \cos(\gamma)] [J_n(kb) + c_n]^2 \quad (90)$$

In the case $\gamma = \pi/2$

$$T = \frac{\mu_0 I^2}{4} \sum_{n=0}^{\infty} n \epsilon_n \sin(n\phi_0) [J_n(kb) + c_n]^2 \quad (91)$$

$$P = \frac{\mu_0 I^2 \omega}{4} \sum_{n=0}^{\infty} \epsilon_n [J_n(kb) + c_n]^2 \quad (92)$$

and

$$M = \frac{\sum_{n=0}^{\infty} n \epsilon_n \sin(n\phi_0) [J_n(kb) + c_n]^2}{\sum_{n=0}^{\infty} \epsilon_n [J_n(kb) + c_n]^2} \quad (93)$$

The expressions for power and torque show similarity with those obtained for the conducting cylinder. It has been already established (eq. (34b)) that

$$\frac{\mu_0 I^2 \omega}{4}$$

is the power radiated by two line sources with a phase difference $\gamma = \pi/2$. Then the term

$$\sum_{n=0}^{\infty} \epsilon_n [J_n(kb) + c_n]^2$$

is due to the influence of the dielectric cylinder. As in the conducting cylinder case this effect becomes negligible if the distance of the antennas from the cylinder is large (see fig. (19)).

The most remarkable change of the torque/power ratio can be noticed when the line sources are close to the cylinder. In fig. (28) there is a small deformation of the curve for $kb = 1.5$. Relative permittivity of the cylinder is 2 in this case. The irregularity becomes more visible if relative permittivity increases to 5 as shown in fig. (29).

The dependence of the torque/power ratio, for $kb = 1.5$ and relative permittivity equal 5, on the spacial angle between the sources is shown in fig. (30). The curve here lost its characteristic shape. As kb increases (assuming that ka stays constant), the distortion is smoothed out and the shape of the curve becomes similar to those given in figures (12) and (24).

Looking over the results of chapters III and IV we can conclude that the supporting constructions which are close to the radiating current filaments will enhance the torque efficiency, if they are suitably arranged. Also, as we have expected, the use of dielectric materials for the

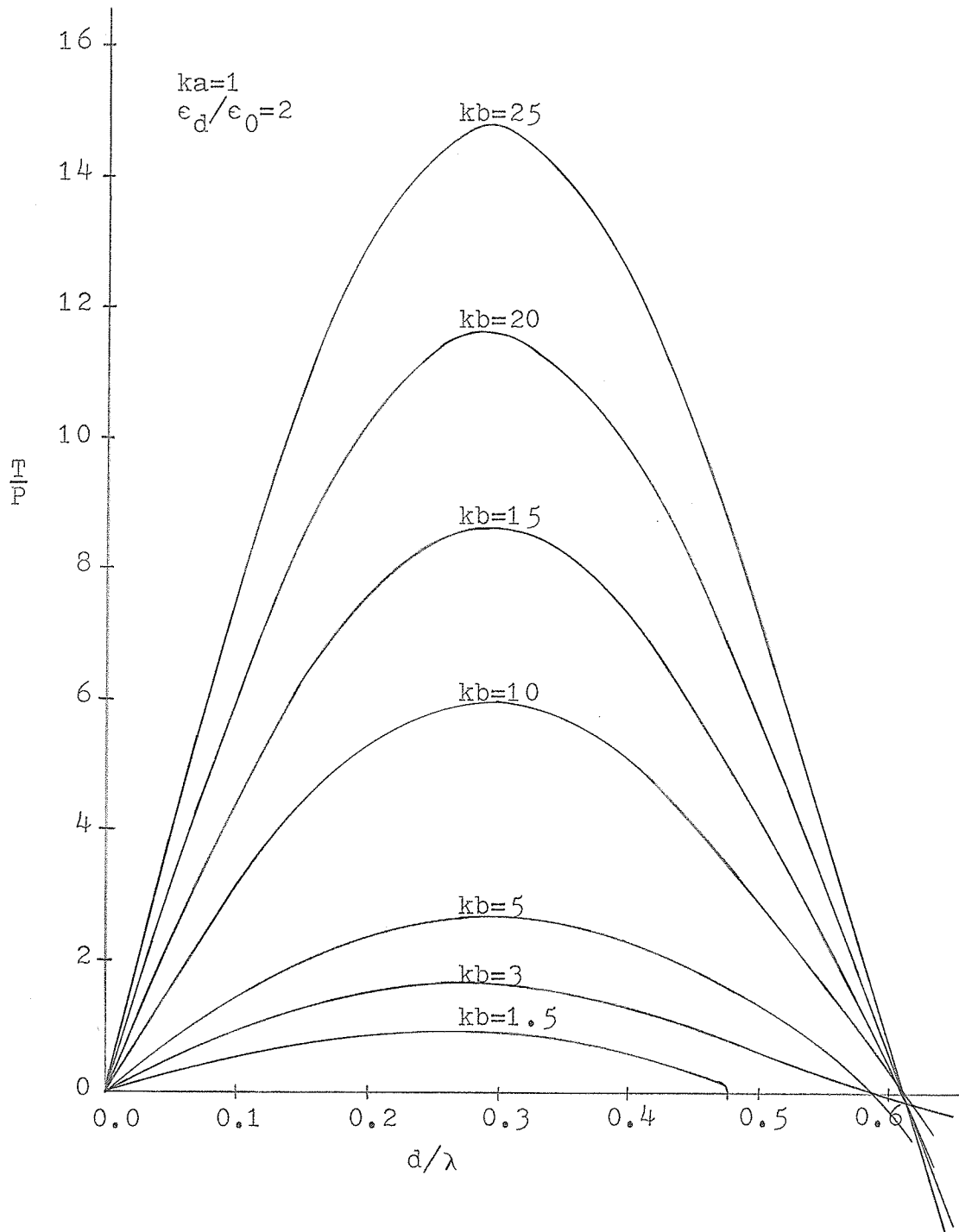


Fig. 28 - Torque/power ratio of two line sources close to a dielectric cylinder

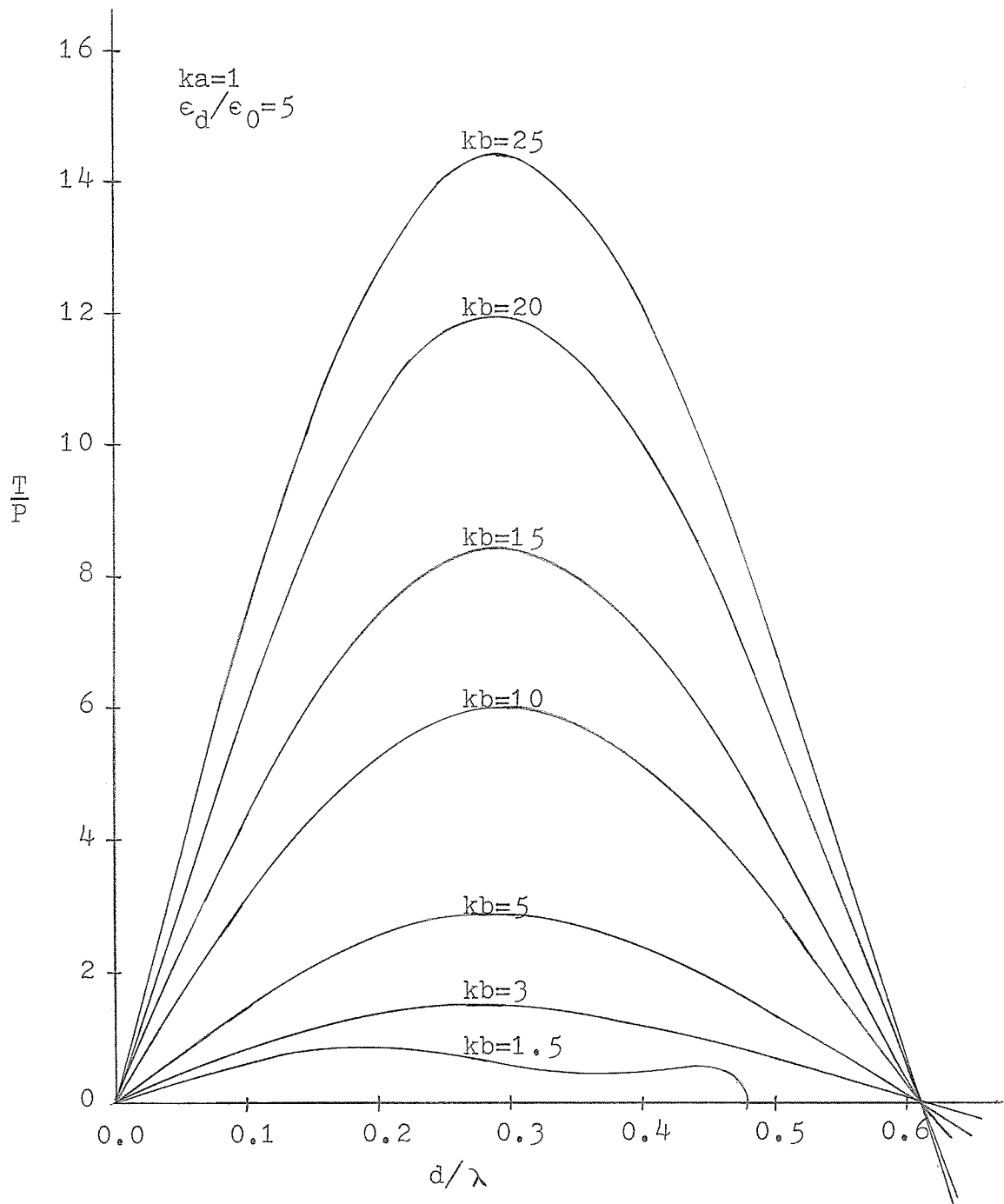


Fig. 29 - Torque/power ratio of two line sources close to a dielectric cylinder

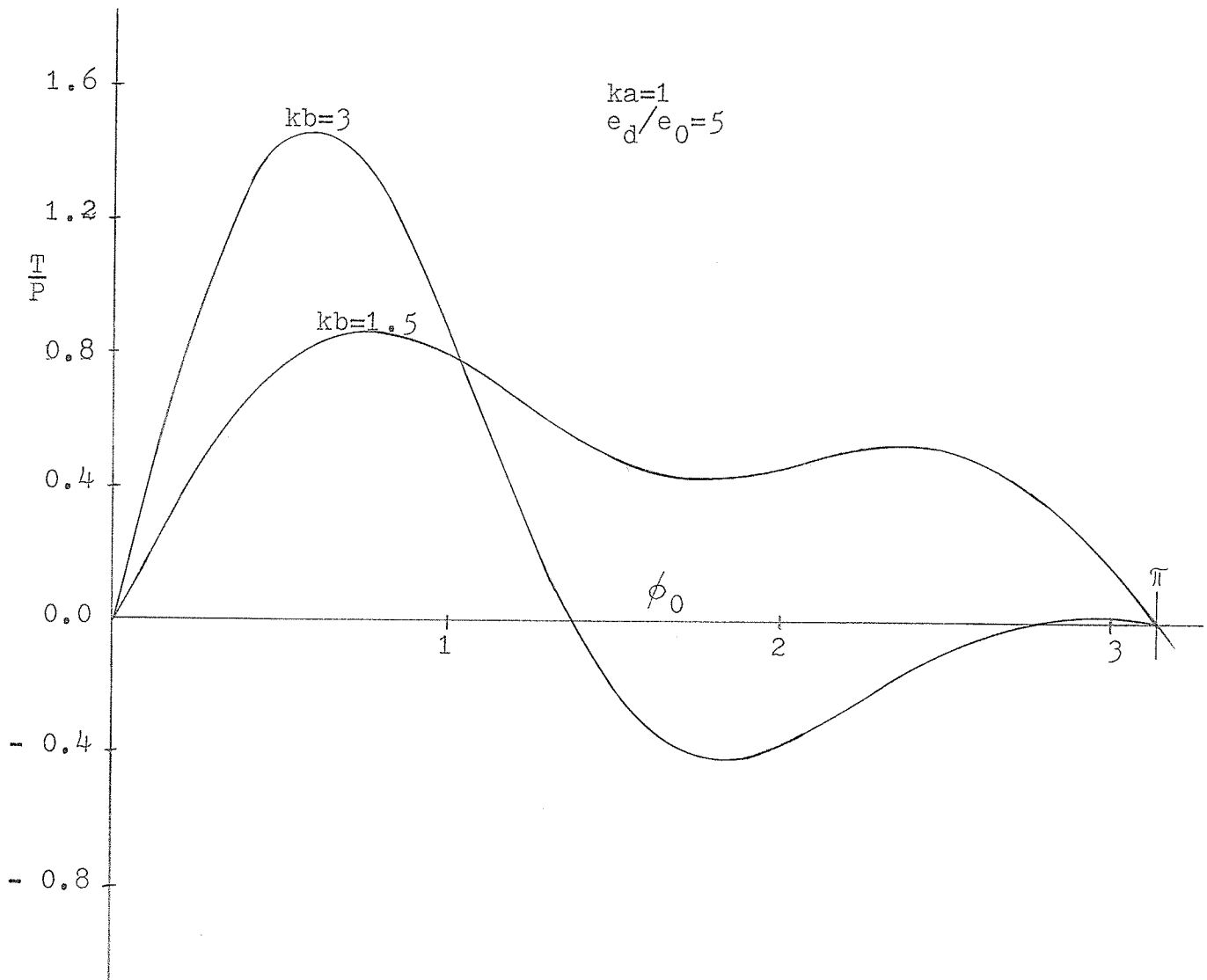


Fig. 30 - Torque/power ratio of two line sources close to a dielectric cylinder

construction helps to increase torque (comparing to torque obtained if conducting supports are used).

Infinite line sources are not easily approximated by real antennas. That is why a more practical investigation would concentrate on radiating dipoles. The following chapters discuss dipoles close to a conducting cylinder (chapter V) and a possibility of producing torque in an arbitrary direction (chapter VI).

V. DIPOLES IN THE PRESENCE OF AN INFINITE CONDUCTING
CYLINDER

So far in the problems discussed the sources of cylindrical waves were used. In this section we will consider the sources of the spherical waves. For that reason eq. (16) will be used for the calculation of torque:

$$\bar{T} = \frac{1}{2} \operatorname{Re} \oint_A \bar{r} \times \left[\epsilon_0 (\bar{E}^* \cdot \bar{n}) \cdot \bar{E} + \frac{1}{\mu_0} (\bar{B}^* \cdot \bar{n}) \cdot \bar{B} \right] dA \quad (16)$$

where A is a spherical surface, the radius of which goes to infinity; also $\bar{n} = \bar{a}_r$.

The mutual arrangement of the two dipoles and of the cylinder is analogous to that of the line sources and the cylinder. Both dipoles are in the x - y plane, parallel to the axis of the cylinder. The distance from the cylinder axis is equal for both dipoles and denoted "b". The arms holding the dipoles are making angle ϕ_0 . (See fig. 31)

Since the boundary of the problem is a cylinder, we will express the incident field in terms of the cylindrical wave functions. The wave function, due to the first dipole in the position shown in fig. 31, is given by:

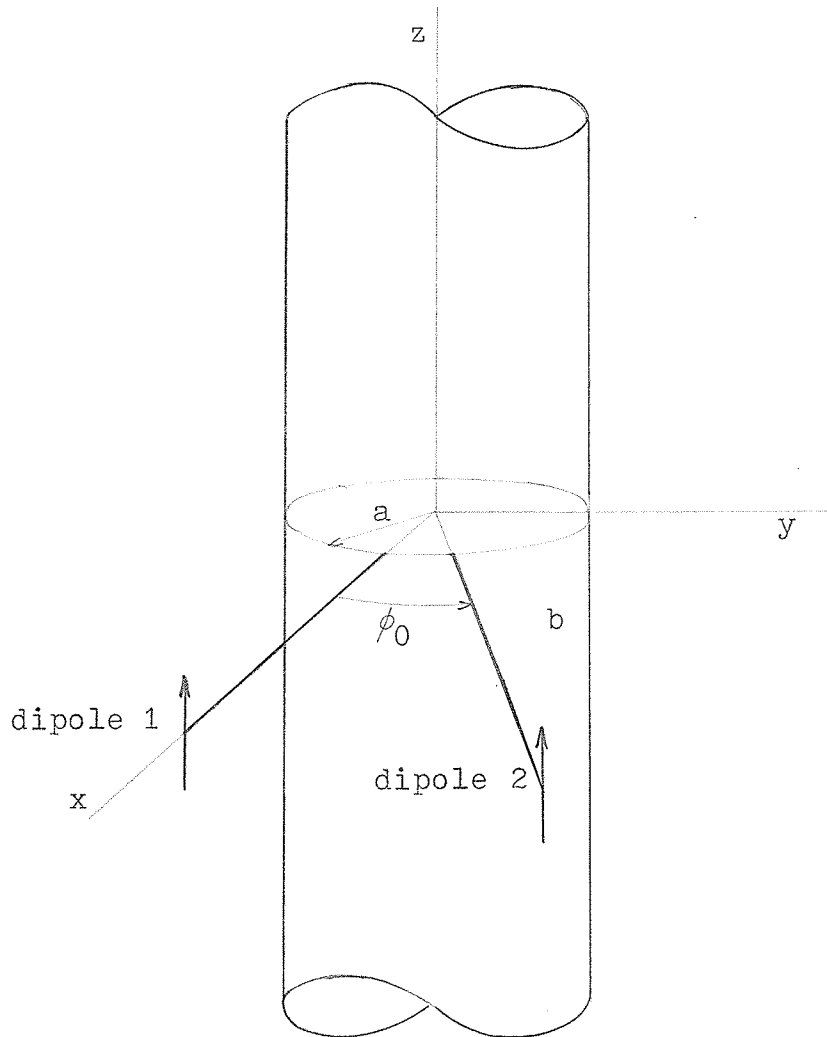


Fig. 31 - Arrangement of two dipoles close to a conducting cylinder

$$\psi_1 = \frac{I_1}{8\pi i} \int_{-\infty}^{\infty} H_0^{(2)}(\beta|\bar{\rho} - \bar{\rho}_0|) \exp(i\alpha z) d\alpha, \quad \beta = (k^2 - \alpha^2)^{1/2}$$

where α is an eigenvalue in the z-direction.

Using the addition theorem

$$\psi_1 = \begin{cases} \frac{I_1}{8\pi i} \int_{-\infty}^{\infty} \sum_{n=-\infty}^{\infty} n J_n(\beta\rho) H_n^{(2)}(\beta b) \exp(in\phi) \exp(i\alpha z) d\alpha & \rho < b \\ \frac{I_1}{8\pi i} \int_{-\infty}^{\infty} \sum_{n=-\infty}^{\infty} n J_n(\beta b) H_n^{(2)}(\beta\rho) \exp(in\phi) \exp(i\alpha z) d\alpha & \rho > b \end{cases} \quad (94)$$

The wave function due to the second dipole is:

$$\psi_2 = \begin{cases} \frac{I_1}{8\pi i} \int_{-\infty}^{\infty} \sum_{n=-\infty}^{\infty} n J_n(\beta\rho) H_n^{(2)}(\beta b) \exp[in(\gamma - \phi_0)] \exp(i\alpha z) d\alpha & \rho < b \\ \frac{I_1}{8\pi i} \int_{-\infty}^{\infty} \sum_{n=-\infty}^{\infty} n J_n(\beta b) H_n^{(2)}(\beta\rho) \exp[in(\gamma - \phi_0)] \exp(i\alpha z) d\alpha & \rho > b \end{cases} \quad (95)$$

The incident wave function is created by superposition of both individual ones:

$$\psi_{\text{inc}} = \begin{cases} \frac{I_1}{8\pi i} \int_{-\infty}^{\infty} \left\{ \exp(i\alpha z) d\alpha \sum_{n=-\infty}^{\infty} \exp(in\phi) H_n^{(2)}(\beta b) J_n(\beta\rho) \cdot [1 + \exp(i\gamma - in\phi_0)] \right\} & \rho < b \\ \frac{I_1}{8\pi i} \int_{-\infty}^{\infty} \left\{ \exp(i\alpha z) d\alpha \sum_{n=-\infty}^{\infty} \exp(in\phi) H_n^{(2)}(\beta\rho) J_n(\beta b) \cdot [1 + \exp(i\gamma - in\phi_0)] \right\} & \rho > b \end{cases} \quad (96)$$

The reflected field is then:

$$\psi_{\text{ref}} = \frac{I l}{8\pi i} \int_{-\infty}^{\infty} \left\{ \exp(i\alpha z) d\alpha \sum_{n=-\infty}^{\infty} \exp(in\phi) A_n H_n^{(2)}(\beta b) H_n^{(2)}(\beta \rho) \cdot [1 + \exp(i\gamma - in\phi_0)] \right. \quad (97)$$

where

$$A_n = - \frac{J_n(\beta a)}{H_n^{(2)}(\beta a)} \quad (98)$$

From the total wave function for $\rho > b$

$$\begin{aligned} \psi_{\text{total}} &= \psi_{\text{inc}} + \psi_{\text{ref}} = \\ &= \frac{I l}{8\pi i} \int_{-\infty}^{\infty} \left\{ \exp(i\alpha z) d\alpha \sum_{n=-\infty}^{\infty} \exp(in\phi) H_n^{(2)}(\beta \rho) K_n(\beta) \cdot [1 + \exp(i\gamma - in\phi_0)] \right\} \quad (99) \end{aligned}$$

the corresponding electric and magnetic fields are found:

$$E_{\rho} = - \frac{I l}{8\pi \epsilon_0 \omega} \int_{-\infty}^{\infty} \left\{ i\alpha \exp(i\alpha z) d\alpha \sum_{n=-\infty}^{\infty} \exp(in\phi) \beta H_n^{(2)}(\beta \rho) \cdot K_n(\beta) [1 + \exp(i\gamma - in\phi_0)] \right\} \quad (100)$$

$$E_{\phi} = \frac{I l}{8\pi \epsilon_0 \omega} \int_{-\infty}^{\infty} \left\{ \alpha \exp(i\alpha z) d\alpha \sum_{n=-\infty}^{\infty} n \exp(in\phi) H_n(\beta \rho) K_n(\beta) \cdot [1 + \exp(i\gamma - in\phi_0)] \right\} \quad (101)$$

$$E_z = - \frac{I l}{8 \pi \epsilon_0 \omega} \int_{-\infty}^{\infty} \left\{ \beta^2 \exp(i \alpha z) d \alpha \sum_{n=-\infty}^{\infty} \exp(in \phi) H_n^{(2)}(\beta \rho) K_n(\beta) \cdot [1 + \exp(i \gamma - in \phi_0)] \right\} \quad (102)$$

$$H_\rho = \frac{I l}{8 \pi \rho} \int_{-\infty}^{\infty} \left\{ \exp(i \alpha z) d \alpha \sum_{n=-\infty}^{\infty} n \exp(in \phi) H_n^{(2)}(\beta \rho) K_n(\beta) \cdot [1 + \exp(i \gamma - in \phi_0)] \right\} \quad (103)$$

$$H_\phi = \frac{I l}{8 \pi i} \int_{-\infty}^{\infty} \left\{ \beta \exp(i \alpha z) d \alpha \sum_{n=-\infty}^{\infty} \exp(in \phi) H_n^{(2)}(\beta \rho) K_n(\beta) \cdot [1 + \exp(i \gamma - in \phi_0)] \right\} \quad (104)$$

$$H_z = 0$$

The above expressions are for the fields at $\rho > b$. $K_n(\beta)$ is defined as:

$$K_n(\beta) = J_n(\beta b) - \frac{J_n(\beta a)}{H_n^{(2)}(\beta a)} H_n^{(2)}(\beta b) \quad (105)$$

The Hankel functions of the second kind and their derivatives for the far field are approximated by:

$$H_n^{(2)}(\beta \rho) \xrightarrow{\beta \rho \rightarrow \infty} \left(\frac{2}{\pi \beta \rho} \right)^{\frac{1}{2}} \exp[-i(\beta \rho - n\pi/2 - \pi/4)]$$

$$H_n^{(2)'}(\beta \rho) \xrightarrow{\beta \rho \rightarrow \infty} \left(\frac{2}{\pi \beta \rho} \right)^{\frac{1}{2}} \exp[-i(\beta \rho - n\pi/2 - \pi/4)]$$

The approximations are substituted into (100) through (104) and by interchanging the order of the summation and integration we can write:

$$E_{\rho} = - \frac{iI_1}{8\pi\epsilon_0\omega} \sqrt{\frac{2}{\pi\rho}} \exp(-i\pi/4) \sum_{n=-\infty}^{\infty} \exp[in(\phi + \pi/2)] [1 + \exp(i\gamma - in\phi_0)] I_1 \quad (106)$$

$$E_{\phi} = \frac{I_1}{8\pi\epsilon_0\omega} \sqrt{\frac{2}{\pi\rho}} \exp(i\pi/4) \sum_{n=-\infty}^{\infty} n \exp[in(\phi + \pi/2)] [1 + \exp(i\gamma - in\phi_0)] I_2 \quad (107)$$

$$E_z = - \frac{I_1}{8\pi\epsilon_0\omega} \sqrt{\frac{2}{\pi\rho}} \exp(i\pi/4) \sum_{n=-\infty}^{\infty} \exp[in(\phi + \pi/2)] [1 + \exp(i\gamma - in\phi_0)] I_3 \quad (108)$$

$$H_{\rho} = \frac{I_1}{8\pi\rho} \sqrt{\frac{2}{\pi\rho}} \exp(i\pi/4) \sum_{n=-\infty}^{\infty} n \exp[in(\phi + \pi/2)] [1 + \exp(i\gamma - in\phi_0)] I_4 \quad (109)$$

$$H_{\phi} = \frac{I_1}{8\pi i} \sqrt{\frac{2}{\pi\rho}} \exp(-i\pi/4) \sum_{n=-\infty}^{\infty} \exp[in(\phi + \pi/2)] [1 + \exp(i\gamma - in\phi_0)] I_5 \quad (110)$$

where

$$\begin{aligned}
 I_1 &= \int_{-\infty}^{\infty} \alpha \beta^{1/2} \exp[i(\alpha z - \beta \rho)] K_n(\beta) d\alpha \\
 I_2 &= \int_{-\infty}^{\infty} \alpha \beta^{-1/2} \exp[i(\alpha z - \beta \rho)] K_n(\beta) d\alpha \\
 I_3 &= \int_{-\infty}^{\infty} \beta^{3/2} \exp[i(\alpha z - \beta \rho)] K_n(\beta) d\alpha \\
 I_4 &= \int_{-\infty}^{\infty} \beta^{-1/2} \exp[i(\alpha z - \beta \rho)] K_n(\beta) d\alpha \\
 I_5 &= \int_{-\infty}^{\infty} \beta^{1/2} \exp[i(\alpha z - \beta \rho)] K_n(\beta) d\alpha
 \end{aligned}$$

To evaluate the integrals I_1 through I_5 , use a substitution:

$$\begin{aligned}
 z &= r \cos \theta & \alpha &= k \cos \chi & d\alpha &= -k \sin \chi d\chi \\
 \rho &= r \sin \theta & \beta &= k \sin \chi
 \end{aligned}$$

The limits of the integrals will change accordingly:

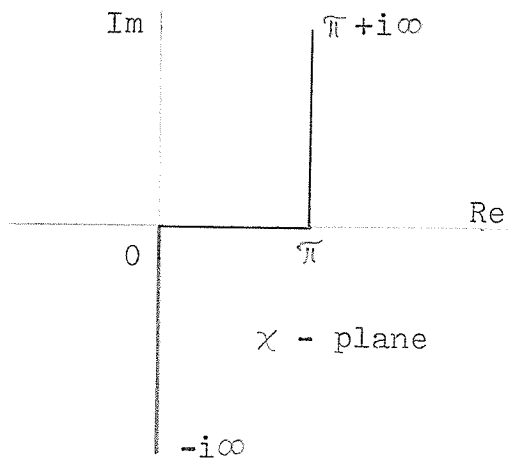
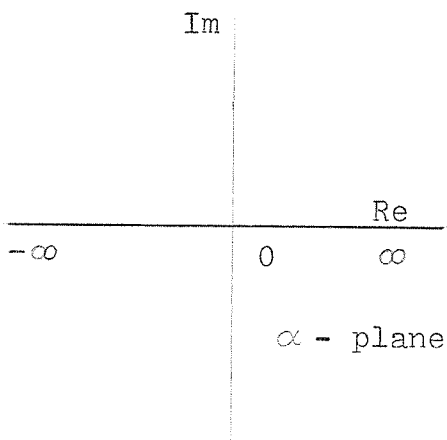


Fig. 32 - Contour of integration in α -plane

Fig. 33 - Contour of integration in χ -plane

if $\alpha \rightarrow \infty$, $\chi \rightarrow -i\infty$

if $\alpha \rightarrow -\infty$, $\chi \rightarrow \pi + i\infty$

The integration path will have shape as shown in fig. (33).

Rewriting the integrals I_1 through I_5 we get:

$$I_1 = - \int_{\pi+i\infty}^{-i\infty} k^{5/2} \cos\chi \sin^{3/2}\chi \exp[ikr \cos(\theta + \chi)] K_n(k \sin\chi) d\chi$$

$$I_2 = - \int_{\pi+i\infty}^{-i\infty} k^{3/2} \cos\chi \sin^{1/2}\chi \exp[ikr \cos(\theta + \chi)] K_n(k \sin\chi) d\chi$$

$$I_3 = - \int_{\pi+i\infty}^{-i\infty} k^{5/2} \sin^{5/2}\chi \exp[ikr \cos(\theta + \chi)] K_n(k \sin\chi) d\chi$$

$$I_4 = - \int_{\pi+i\infty}^{-i\infty} k^{1/2} \sin^{1/2}\chi \exp[ikr \cos(\theta + \chi)] K_n(k \sin\chi) d\chi$$

$$I_5 = - \int_{\pi+i\infty}^{-i\infty} k^{3/2} \sin^{3/2}\chi \exp[ikr \cos(\theta + \chi)] K_n(k \sin\chi) d\chi$$

The asymptotic values of these integrals for the far field is found by the "method of steepest descent". (12)

Setting

$$f(\chi) = \cos(\theta + \chi) \quad (111)$$

the saddle point is found from

$$\frac{df(\chi)}{d\chi} = -\sin(\theta + \chi) = 0 \quad (112)$$

Condition (112) gives a series of acceptable points:

$$\chi = n\pi - \theta \quad n = 0, 1, 2, 3, \dots$$

from which the point for $n = 0$ is chosen, so that

$$\chi = -\theta$$

Using eq. (4) given by Jones⁽¹²⁾ on p. 445 we finally have:

$$I_1 = \left[-\frac{2}{ikr} \right]^{1/2} k^{5/2} \cos\theta \sin^{3/2}\theta K_n(k \sin\theta) \exp(-ikr) \quad (113)$$

$$I_2 = \left[-\frac{2}{ikr} \right]^{1/2} k^{3/2} \cos\theta \sin^{1/2}\theta K_n(k \sin\theta) \exp(-ikr) \quad (114)$$

$$I_3 = -\left[-\frac{2}{ikr} \right]^{1/2} k^{5/2} \sin^{5/2}\theta K_n(k \sin\theta) \exp(-ikr) \quad (115)$$

$$I_4 = -\left[-\frac{2}{ikr} \right]^{1/2} k^{1/2} \sin^{1/2}\theta K_n(k \sin\theta) \exp(-ikr) \quad (116)$$

$$I_5 = - \left[- \frac{2}{ikr} \right]^{1/2} k^{3/2} \sin^{3/2} \theta K_n(k \sin \theta) \exp(-ikr) \quad (117)$$

By substitution of (113) through (117) into (106) through (110) we get the approximate expressions for the far fields in forms:

$$E_\rho = - \frac{ik^2 I_1}{4\pi \epsilon_0 \omega r} \exp(-ikr) \cos \theta \sin \theta \sum_{n=-\infty}^{\infty} \exp[in(\phi + \pi/2)] \cdot K_n(k \sin \theta) [1 + \exp(i\gamma - in\phi_0)] \quad (118)$$

$$E_\phi = \frac{ik I_1}{4\pi \epsilon_0 \omega r^2} \exp(-ikr) \frac{\cos \theta}{\sin \theta} \sum_{n=-\infty}^{\infty} n \exp[in(\phi + \pi/2)] \cdot K_n(k \sin \theta) [1 + \exp(i\gamma - in\phi_0)] \quad (119)$$

$$E_z = \frac{ik^2 I_1}{4\pi \epsilon_0 \omega r} \exp(-ikr) \sin^2 \theta \sum_{n=-\infty}^{\infty} \exp[in(\phi + \pi/2)] K_n(k \sin \theta) \cdot [1 + \exp(i\gamma - in\phi_0)] \quad (120)$$

$$H_\rho = - \frac{i I_1}{4\pi \rho r} \exp(-ikr) \sum_{n=-\infty}^{\infty} n \exp[in(\phi + \pi/2)] K_n(k \sin \theta) \cdot [1 + \exp(i\gamma - in\phi_0)] \quad (121)$$

$$H_\phi = - \frac{ik I_1}{4\pi r} \exp(-ikr) \sin \theta \sum_{n=-\infty}^{\infty} \exp[in(\phi + \pi/2)] K_n(k \sin \theta) \cdot [1 + \exp(i\gamma - in\phi_0)] \quad (122)$$

$K_n(k \sin\theta)$, similarly as in (105) stands for

$$K_n(k \sin\theta) = J_n(kb \sin\theta) - \frac{J_n(ka \sin\theta)}{H_n^{(2)}(ka \sin\theta)} H_n^{(2)}(kb \sin\theta) \quad (123)$$

From equation (16) the components of torque in ρ , ϕ and z directions are found:

$$T_\rho = -\frac{1}{2} \operatorname{Re} \int_0^\pi \int_0^{2\pi} \rho \cos\theta [\epsilon_0 (E_\rho^* \sin\theta + E_z^* \cos\theta) E_\phi + \mu_0 H_\rho^* H_\phi \sin\theta] r^2 \sin\theta d\phi d\theta \quad (124)$$

$$T_\phi = \frac{1}{2} \operatorname{Re} \int_0^\pi \int_0^{2\pi} \rho \left\{ \cos\theta [\epsilon_0 (E_\rho^* \sin\theta + E_z^* \cos\theta) E_\rho + \mu_0 H_\rho^* H_\rho] + \sin\theta [\epsilon_0 (E_\rho^* \sin\theta + E_z^* \cos\theta) E_z] \right\} r^2 \sin\theta d\phi d\theta \quad (125)$$

$$T_z = \frac{1}{2} \operatorname{Re} \int_0^\pi \int_0^{2\pi} \rho \sin\theta \left\{ \epsilon_0 (E_\rho^* \sin\theta + E_z^* \cos\theta) E_\phi + \mu_0 H_\rho^* H_\phi \sin\theta \right\} r^2 \sin\theta d\phi d\theta \quad (126)$$

The relations for the electric and magnetic fields are substituted, and as in the previous chapters the integration over the range of ϕ is:

$$\int_0^{2\pi} \exp[i(n-m)\phi] d\phi = \begin{cases} 0 & n \neq m \\ 2\pi & n = m \end{cases}$$

After the indicated operations are carried through,

we find:

$$T_{\rho} = - \frac{k^3 I_1^2 l^2}{8\pi\omega^2 \epsilon_0} \sum_{n=-\infty}^{\infty} n [1 + \cos(\gamma - n\phi_0)] \int_0^{\pi} \sin^3 \theta \cos \theta [K_n(r \sin \theta)]^2 d\theta \quad (127)$$

$$T_{\phi} = \frac{k^2 I_1^2 l^2}{8\pi\omega^2 \epsilon_0} \sum_{n=-\infty}^{\infty} n^2 [1 + \cos(\gamma - n\phi_0)] \int_0^{\pi} \sin \theta \cos \theta [K_n(r \sin \theta)]^2 d\theta \quad (128)$$

$$T_z = - \frac{k^2 I_1^2 l^2}{8\pi\omega^2 \epsilon_0} \sum_{n=-\infty}^{\infty} n [1 + \cos(\gamma - n\phi_0)] \int_0^{\pi} \sin^3 \theta [K_n(r \sin \theta)]^2 d\theta \quad (129)$$

Let us define an integral J as

$$J = \int_0^{\pi} f(\sin \theta) \cos \theta d\theta \quad (130)$$

$f(\sin \theta)$ is a suitably regular function on the interval $(0, \pi)$.

Since

$$\sin \theta = \sin(\pi - \theta)$$

and

$$\cos \theta = - \cos(\pi - \theta)$$

we can also write

$$f(\sin \theta) = f[\sin(\pi - \theta)]$$

Generally the integration can be divided in the following

manner:

$$J = \int_0^{\pi/2} f(\sin\theta) \cos\theta \, d\theta + \int_{\pi/2}^{\pi} f(\sin\theta) \cos\theta \, d\theta \quad (131)$$

Now in the second part on the righthand side of (131) let

$\theta \longrightarrow \pi - \theta$ so that

$$\begin{aligned} \int_{\pi/2}^{\pi} f(\sin\theta) \cos\theta \, d\theta &= - \int_{\pi/2}^0 f[\sin(\pi - \theta) \cos(\pi - \theta)] \, d\theta = \\ &= - \int_0^{\pi/2} f(\sin\theta) \cos\theta \, d\theta \end{aligned} \quad (132)$$

It follows that

$$J = 0$$

The integrals contained in the equations (127) and (128) are of the same nature, therefore

$$\left. \begin{aligned} T_\rho &= 0 \\ T_\phi &= 0 \end{aligned} \right\} \quad (133)$$

We have only one component of torque left; the torque magnitude is then given by eq. (129).

$$T = \frac{k^3 I_1^2 l^2}{8\pi\omega^2 \epsilon_0} \sum_{n=0}^{\infty} n \epsilon_n \int_0^{\pi} \sin^3 \theta [K_n(r \sin \theta)]^2 d\theta \quad (138)$$

$$P = \frac{k^3 I_1^2 l^2}{8\pi\omega \epsilon_0} \sum_{n=0}^{\infty} \epsilon_n \int_0^{\pi} \sin^3 \theta [K_n(r \sin \theta)]^2 d\theta \quad (139)$$

Power radiated by two dipoles is given by

$$P = \frac{k^3 I_1^2 l^2}{6\pi\omega \epsilon_0}$$

The reduction of equation (139) if $ka = 0$ leads to the same expression. The relative value of power for $\gamma = \pi/2$ is shown in fig. 32. As the distance of the dipoles from the cylinder increases, the influence of the cylinder decreases; for large values of kb the value of power is that of the two dipoles in free space.

The torque/power ratio curves retain the same character as it was in the case of the line sources - see fig.'s (33) and (34). From Chute⁽⁷⁾ the approximate value of the torque/power ratio of two dipoles in free space is

$$\frac{T}{P} \approx 0.476 \frac{kbc \cos(\phi_0/2)}{\omega} \quad (140)$$

(see Appendix)

To calculate the radiated power we will start from eq. (18). Decomposition of the fields into their components in the cylindrical coordinates will change the form of eq. (18) to:

$$P = \frac{1}{2} \operatorname{Re} \int_0^{\pi} \int_0^{2\pi} r^2 \sin\theta [-E_z H_\phi^* + (E_\rho H_\theta^* - E_\theta H_\rho^*) \cos\theta] d\phi d\theta \quad (134)$$

By the same procedure as for the torque calculations we get

$$P = \frac{k^3 I_1^2 \omega^2}{8\pi \epsilon_0 \omega} \sum_{n=-\infty}^{\infty} [1 + \cos(\gamma - n\phi_0)] \int_0^{\pi} \sin^3\theta [K_n(r \sin\theta)]^2 d\theta \quad (135)$$

Replacing the summation from $-\infty$ to ∞ in eq.'s (129) and (135) by the summation from 0 to ∞ yields:

$$T = \frac{k^3 I_1^2 \omega^2}{8\pi \omega^2 \epsilon_0} \sin\gamma \sum_{n=0}^{\infty} n \epsilon_n \int_0^{\pi} \sin^3\theta [K_n(r \sin\theta)]^2 d\theta \quad (136)$$

$$P = \frac{k^3 I_1^2 \omega^2}{8\pi \omega \epsilon_0} \sum_{n=0}^{\infty} \epsilon_n [(1 + \cos\gamma \cos n\phi_0)] \int_0^{\pi} \sin^3\theta [K_n(r \sin\theta)]^2 d\theta \quad (137)$$

For the special case of phase difference $\gamma = \pi/2$ torque and power are given by:

This value was obtained for $\gamma = \pi/2$, $d/\lambda = 1/4$. From the fig. 34 for $\phi_0 = 5.08$ radians, $kb = 1.4$ we obtain

$$\frac{T}{P} \approx 0.649 \frac{1}{\omega} \quad (141)$$

If we substitute ϕ_0 and kb in (140):

$$\frac{T}{P} = 0.55 \frac{1}{\omega} \quad (142)$$

Considering the approximations Chute used in his derivations, the agreement is good.

In the actual applications, control of only torque magnitude would hinder any effective attempts of stabilizing a space vehicle, since the direction of disturbing torque is unpredictable. We will consider a production of torque in an arbitrary direction in the following chapter VI.

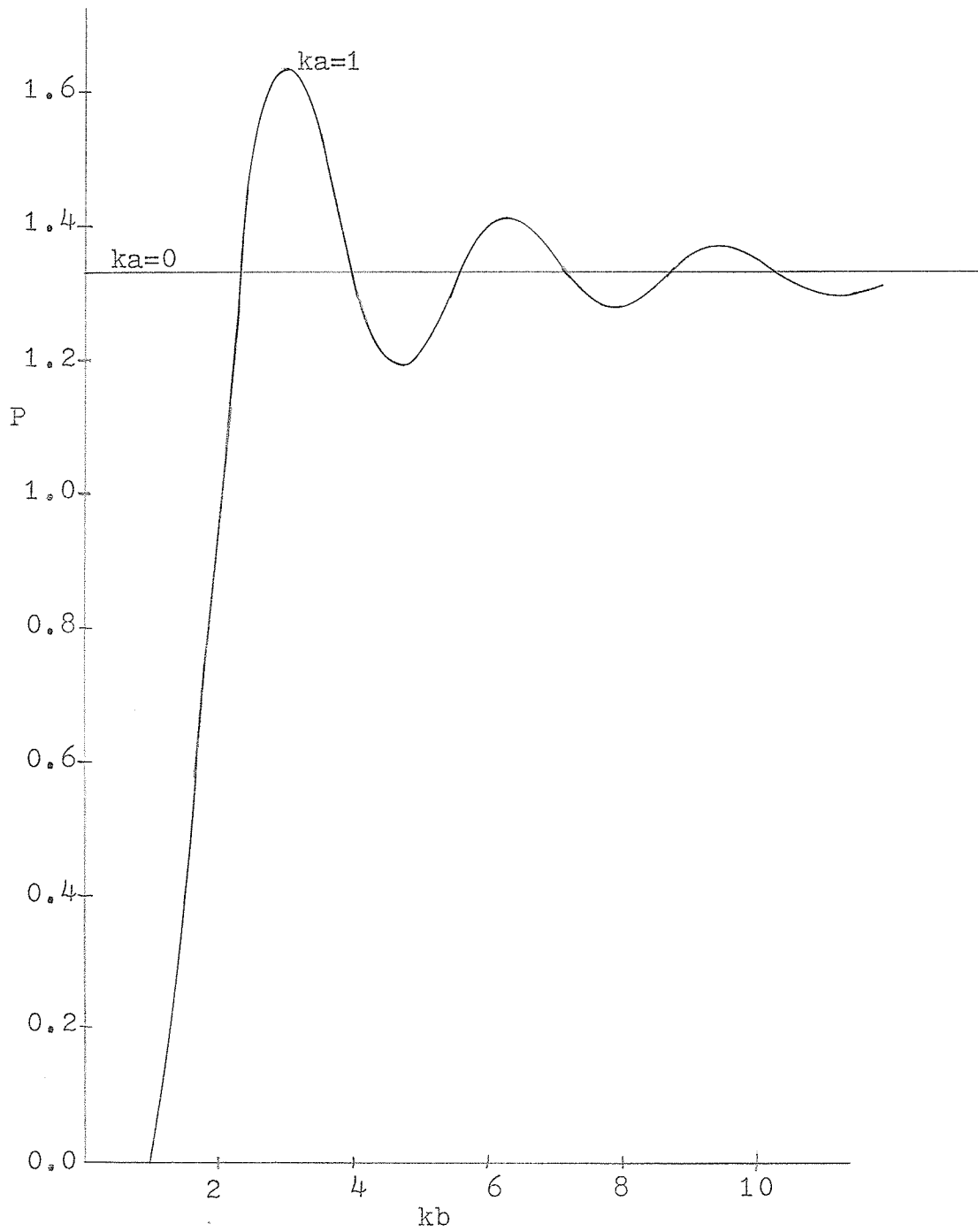


Fig. 34 - Power radiated by two dipoles close to a conducting cylinder

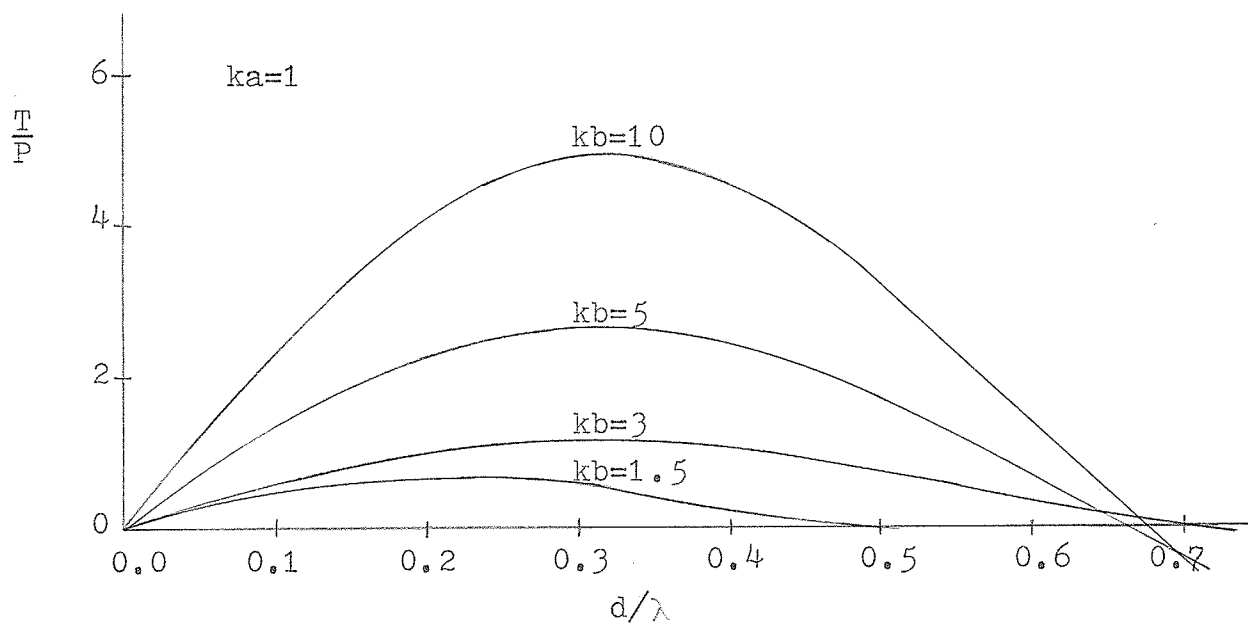


Fig. 35 - Torque/power ratio of two dipoles close to a conducting cylinder

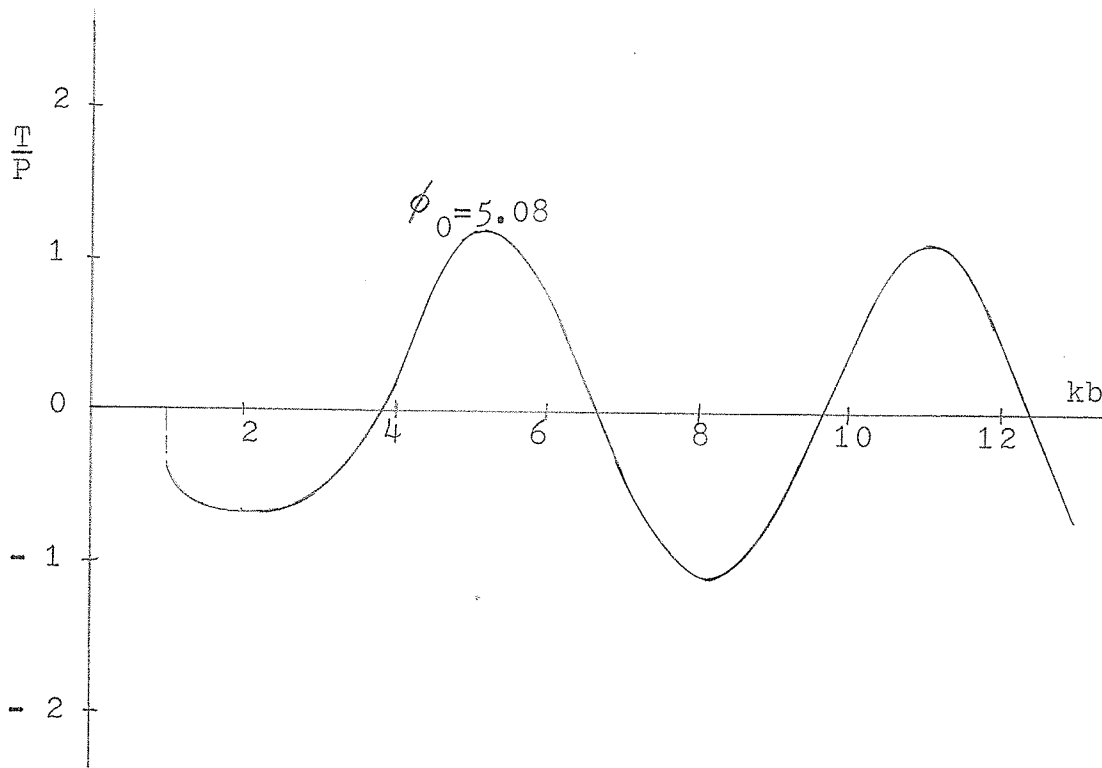


Fig. 36 - Torque/power ratio of two dipoles close to a conducting cylinder.

VI. TORQUE IN AN ARBITRARY DIRECTION

The arrangements of the sources in the previous chapters were such that the only non-zero component of torque was in the z - direction. It is nevertheless possible, by choosing the proper type and configuration of antennas, to produce torque in an arbitrary direction. To show this, we will go back to an antenna located in a free space. The extension to the cases of antennas placed near a supporting element can be carried out similarly.

Most of the works discussing the torque caused by the antenna radiation start with an investigation of a turnstile antenna. The relation between the radiated power and the reactive torque is usually given by:

$$\bar{T} = \frac{1}{\omega} P \quad (143)$$

torque being perpendicular to the plane in which the antenna lies. (6), (7) (See fig. 35)

By adding a third dipole and changing the phase and the magnitude of the currents and the spacial angles of the dipoles, torque in an arbitrary direction can be produced.

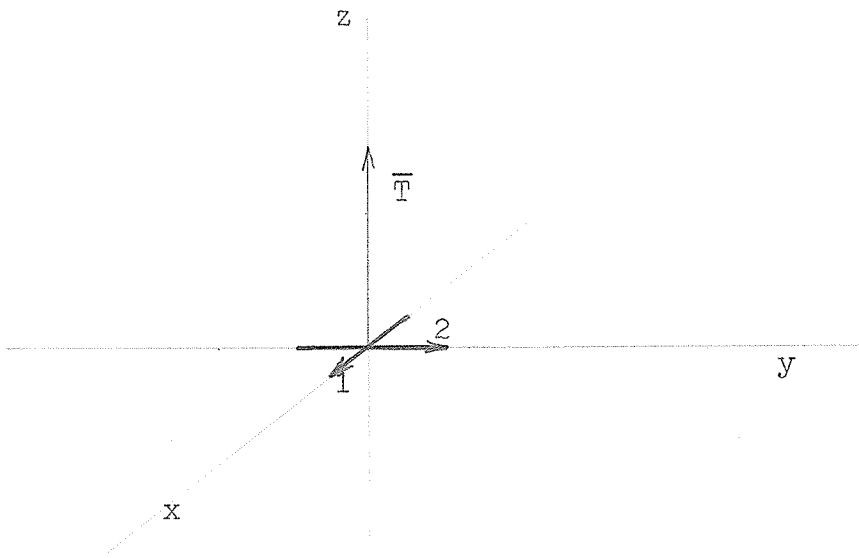


Fig. 37 - Turnstile antenna

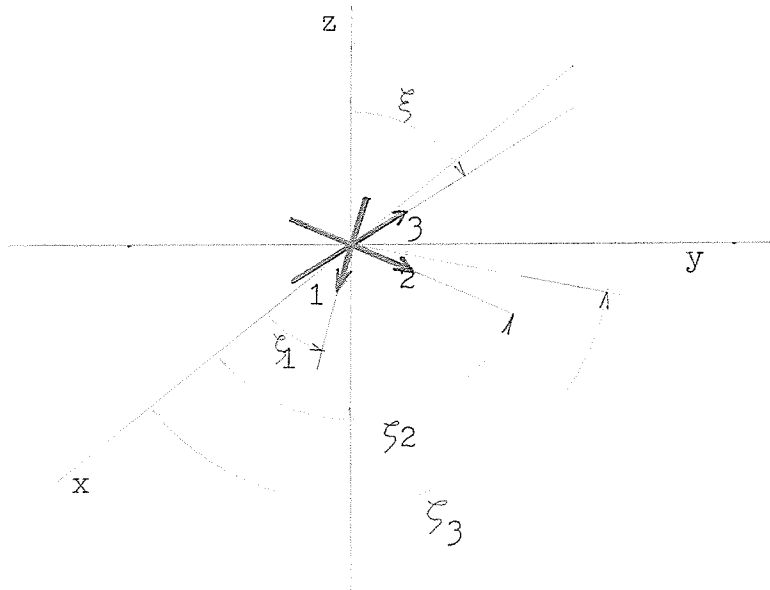


Fig. 38 - Three crossed dipoles

The configuration of fig. 36 is considered. The currents of the individual dipoles are:

$$I_1 = I$$

$$I_2 = I \exp(i\gamma)$$

$$I_3 = I \exp(i\nu)$$

The vector magnetic potentials due to each dipole separately are given by:

$$\bar{A}_1 = \frac{\mu_0 I \bar{I}_1}{4\pi r} \exp(-ikr) \quad (144)$$

$$\bar{A}_2 = \frac{\mu_0 I \bar{I}_2}{4\pi r} \exp(i\gamma - ikr) \quad (145)$$

$$\bar{A}_3 = \frac{\mu_0 I \bar{I}_3}{4\pi r} \exp(i\nu - ikr) \quad (146)$$

From fig. 36 we see that

$$\begin{aligned} \bar{I}_1 &= \bar{I} (\bar{a}_x \cos \zeta_1 + \bar{a}_y \sin \zeta_1) \\ \bar{I}_2 &= \bar{I} (\bar{a}_x \cos \zeta_2 + \bar{a}_y \sin \zeta_2) \\ \bar{I}_3 &= \bar{I} (\bar{a}_x \cos \xi \cos \zeta_3 + \bar{a}_y \cos \xi \sin \zeta_3 + \bar{a}_z \sin \xi) \end{aligned} \quad (147)$$

The total magnetic potential is a superposition of the individual ones:

$$\bar{A} = \bar{A}_1 + \bar{A}_2 + \bar{A}_3 \quad (148)$$

Its components in r , θ and ϕ directions are:

$$A_r = \frac{\mu_0 I l}{4\pi r} \exp(-ikr) \left\{ \sin\theta [\cos(\phi - \zeta_1) + \exp(i\gamma) \cos(\phi - \zeta_2)] + \right. \\ \left. + \exp(i\gamma) [\cos\xi \sin\theta \cos(\phi - \zeta_3) - \sin\xi \cos\theta] \right\} \quad (149)$$

$$A_\theta = \frac{\mu_0 I l}{4\pi r} \exp(-ikr) \left\{ \cos\theta [\cos(\phi - \zeta_1) + \exp(i\gamma) \cos(\phi - \zeta_2)] + \right. \\ \left. + \exp(i\gamma) \cos\xi \cos\theta \cos(\phi - \zeta_3) - \sin\xi \sin\theta \right\} \quad (150)$$

$$A_\phi = \frac{\mu_0 I l}{4\pi r} \exp(-ikr) [\sin(\zeta_1 - \phi) + \exp(i\gamma) \sin(\zeta_2 - \phi) + \\ + \exp(i\gamma) \cos\xi \sin(\zeta_3 - \phi)] \quad (151)$$

The magnetic and electric fields are obtained from the relation

$$\bar{B} = \text{rot } \bar{A} \quad (152)$$

and from Maxwell equation

$$\bar{E} = \frac{1}{i\omega\epsilon_0\mu_0} \text{rot } \bar{B} \quad (153)$$

Usage of eq. (152) gives the components of the magnetic field:

$$B_r = 0$$

$$B_\theta = \frac{\mu_0 I l}{4\pi r} \exp(-ikr) \left(\frac{1}{r} + ik\right) [\sin(\zeta_1 - \phi) + \exp(i\gamma) \sin(\zeta_2 - \phi) + \exp(i\nu) \cos \xi \sin(\zeta_3 - \phi)] \quad (154)$$

$$B_\phi = -\frac{\mu_0 I l}{4\pi r} \exp(-ikr) \left(\frac{1}{r} + ik\right) \left\{ \cos \theta \cos(\zeta_1 - \phi) + \exp(i\gamma) \cdot \cos \theta \cos(\zeta_2 - \phi) + \exp(i\nu) [\cos \xi \cos \theta \cos(\zeta_3 - \phi) - \sin \xi \sin \theta] \right\} \quad (155)$$

From eq. (153) the components of the electric field are derived:

$$E_r = -\frac{i I l}{2\pi \omega \epsilon_0 r^2} \exp(-ikr) \left(\frac{1}{r} + ik\right) \left\{ \sin \theta \cos(\zeta_1 - \phi) + \exp(i\gamma) \sin \theta \cos(\zeta_2 - \phi) + \exp(i\nu) [\sin \xi \cos \theta + \cos \xi \cos(\zeta_3 - \phi) \sin \theta] \right\} \quad (156)$$

$$E_\theta = -\frac{i I l}{4\pi \omega \epsilon_0 r} \exp(-ikr) \left(k^2 - \frac{1}{r^2} - i \frac{k}{r}\right) \left\{ \cos \theta \cos(\zeta_1 - \phi) + \right.$$

$$+ \exp(i\gamma) \cos \theta \cos(\zeta_2 - \phi) + \exp(i\nu) [\cos \xi \cos \theta \cos(\zeta_3 - \phi) - \sin \xi \sin \theta] \} \quad (157)$$

$$E_\phi = - \frac{iIl}{4\pi\omega\epsilon_0 r} \left(k^2 - \frac{1}{r^2} - i \frac{k}{r} \right) [\sin(\zeta_1 - \phi) + \exp(i\gamma) \sin(\zeta_2 - \phi) + \exp(i\nu) \cos \xi \sin(\zeta_3 - \phi)] \exp(-ikr) \quad (158)$$

Torque is given by eq. (16). From it the components in r, θ and ϕ directions are:

$$T_r = 0$$

$$T_\theta = - \frac{\epsilon_0}{2} \text{Re} \int_0^\pi \int_0^{2\pi} r^3 \sin \theta E_r^* E_\phi d\phi d\theta \quad (159)$$

$$T_\phi = \frac{\epsilon_0}{2} \text{Re} \int_0^\pi \int_0^{2\pi} r^3 \sin \theta E_r^* E_\theta d\phi d\theta \quad (160)$$

or, since the cartesian coordinates are more descriptive:

$$T_x = - \frac{\epsilon_0 r^3}{2} \text{Re} \int_0^\pi \int_0^{2\pi} (\sin \theta \cos \theta \cos \phi E_r^* E_\phi + \sin \theta \sin \phi E_r^* E_\theta) d\phi d\theta \quad (161)$$

$$T_y = \frac{\epsilon_0 r^3}{2} \operatorname{Re} \int_0^\pi \int_0^{2\pi} (-\sin\theta \cos\theta \sin\phi E_r^* E_\phi + \sin\theta \cos\phi E_r^* E_\theta) d\phi d\theta \quad (162)$$

$$T_z = \frac{\epsilon_0 r^3}{2} \operatorname{Re} \int_0^\pi \int_0^{2\pi} \sin^2\theta E_r^* E_\phi d\phi d\theta \quad (163)$$

After the substitution of equations (154) through (158) into the relations above, we obtain:

$$T_x = \frac{k^3 I_1^2 l^2}{6\pi\omega^2 \epsilon_0} \sin\xi \sin\xi_1 \sin\nu + \sin\xi \sin\xi_2 \sin(\nu - \gamma) \quad (164)$$

$$T_y = -\frac{k^3 I_1^2 l^2}{6\pi\omega^2 \epsilon_0} [\sin\xi \cos\xi_1 \sin\nu + \sin\xi \cos\xi_2 \sin(\nu - \gamma)] \quad (165)$$

$$T_z = -\frac{k^3 I_1^2 l^2}{6\pi\omega^2 \epsilon_0} [\sin(\xi_2 - \xi_1) \sin\gamma + \cos\xi \sin(\xi_3 - \xi_1) \sin\nu + \cos\xi \sin(\xi_3 - \xi_2) \sin(\nu - \gamma)] \quad (166)$$

The position of the first dipole will be used as a reference; hence we will assign $\xi_1 = 0$. Now

$$T_x = \frac{k^3 I_1^2 l^2}{6\pi\omega^2 \epsilon_0} \sin\xi \sin\xi_2 \sin(\nu - \gamma) \quad (167)$$

$$T_y = - \frac{k^3 I_1^2 l^2}{6\pi\omega^2 \epsilon_0} \sin \xi [\sin \nu + \cos \xi_2 \sin(\nu - \gamma)] \quad (168)$$

$$T_z = - \frac{k^3 I_1^2 l^2}{6\pi\omega^2 \epsilon_0} [\sin \xi_2 \sin \gamma + \cos \xi \sin \xi_3 \sin \nu + \cos \xi \sin(\xi_3 - \xi_2) \sin(\nu - \gamma)] \quad (169)$$

From eq. 15, power radiated by this type of antenna is:

$$P = \frac{1}{2} \operatorname{Re} \int_0^\pi \int_0^{2\pi} r^2 \sin \theta (E_\theta H_\phi^* - H_\theta^* E_\phi) d\phi d\theta \quad (170)$$

which gives:

$$P = \frac{k^3 I_1^2 l^2}{6\pi\omega \epsilon_0} \left[\frac{3}{2} + \cos \xi_2 \cos \gamma + \cos \xi \cos \xi_3 \cos \nu + \cos \xi \cos(\xi_3 - \xi_2) \cos(\nu - \gamma) + \frac{3}{8} \cos^2 \xi \right] \quad (171)$$

The simplest arrangement of the dipoles is shown in fig. 35. That means that $\xi = \pi/2$, $\xi_2 = \pi/2$. The resulting torque and power are then:

$$T_x = \frac{k^3 I_1^2 l^2}{6\pi\omega^2 \epsilon_0} \sin(\nu - \gamma) \quad (172)$$

$$T_y = - \frac{k^3 I_1^2 l^2}{6\pi\omega^2 \epsilon_0} \sin \nu \quad (173)$$

$$T_z = - \frac{k^3 I_1^2 l^2}{6\pi\omega^2 \epsilon_0} \sin \gamma \quad (174)$$

$$P = \frac{k^3 I_1^2 I_2^2}{4\pi r \epsilon_0} \quad (175)$$

From eq.'s (172) through (174) it can be seen that the z component of the torque is due to the interaction of the two dipoles in the x - y plane (γ is the phase difference between dipole 1 and dipole 2). This result is in agreement with those given by F. S. Chute⁽⁷⁾ and P. Bruscaioni, A. Consortini and G. Toraldo di Francia⁽⁶⁾ for two dipole turnstile antenna. Also, comparing (174) to the expressions obtained in the preceding chapters for the line sources and the dipoles in the presence of an infinite cylinder, there is the same sinusoidal dependence on the phase difference γ . It is worthwhile to point out that the value of the z component of torque will not change if the third dipole is completely removed. However, this act would result in the elimination of the other two components given by (172) and (173). The T_x component arises from the interaction between dipole 2 and 3 and T_y is due to the interaction between 1 and 3. It is therefore obvious that the direction of torque can be changed by adjusting the mutual phase differences between the currents in the individual dipoles.

To find the torque/power ratio we need to find the magnitude of torque. It is defined by:

$$T = (T_x^2 + T_y^2 + T_z^2)^{1/2} \quad (176)$$

If the expressions for T_x , T_y and T_z are substituted, the torque magnitude has

$$T = \frac{k^3 I_1^2 l^2}{6\pi\omega^2 \epsilon_0} [\sin^2(\nu - \gamma) + \sin^2\nu + \sin^2\gamma]^{1/2} \quad (177)$$

Then

$$M = \frac{2}{3} [\sin^2(\nu - \gamma) + \sin^2\nu + \sin^2\gamma]^{1/2} \quad (178)$$

In the following case the currents are mutually shifted 120° , i.e. $\gamma = 120^\circ$, $\nu = 240^\circ$. The torque/power ratio is the same as for the two dipole turnstile antenna:

$$\frac{T}{P} = \frac{1}{\omega} \quad (179)$$

It is also the maximum ratio that can be obtained for the discussed set up.

Another arrangement is for example $\gamma = \pi/2$, $\nu = \pi/2$.

It follows that

$$\frac{T}{P} = 0.9428 \frac{1}{\omega} \quad (180)$$

A little different approach would keep the phase differences constant, say $\gamma = 120^\circ$, $\nu = 240^\circ$, leaving the position angle variable.

VII. CONCLUSION

The object of this thesis was to find the relation between reactional torque and radiated power of antenna configurations, both in free space and close to a supporting element. Also attention was paid to the possibility of producing torque about an arbitrary axis.

It was found that a supporting structure, simulated by a circular cylinder in this investigation, may under certain conditions enhance the torque efficiency of the antenna. At the same time, the power efficiency stays unaffected or decreases. This effect is stronger in the case of the dielectric cylinder. Torque and power of the dipole antennas close to a conducting cylinder display similar behaviour to torque and power produced by the line sources. This becomes important if the usage of dipole antennas for control of the attitude of a spaceship is considered. In any case, as the available power on a spaceship and the size of the antennas used for communication and other purposes increase, the reactional torque may be the cause of undesired disturbances which should be taken into account.

APPENDIX

A BEAM RADIATOR⁽⁷⁾

Consider an antenna consisting of two Hertz elements separated by a distance $\lambda/4$. The phase difference of the elements is $\pi/2$.

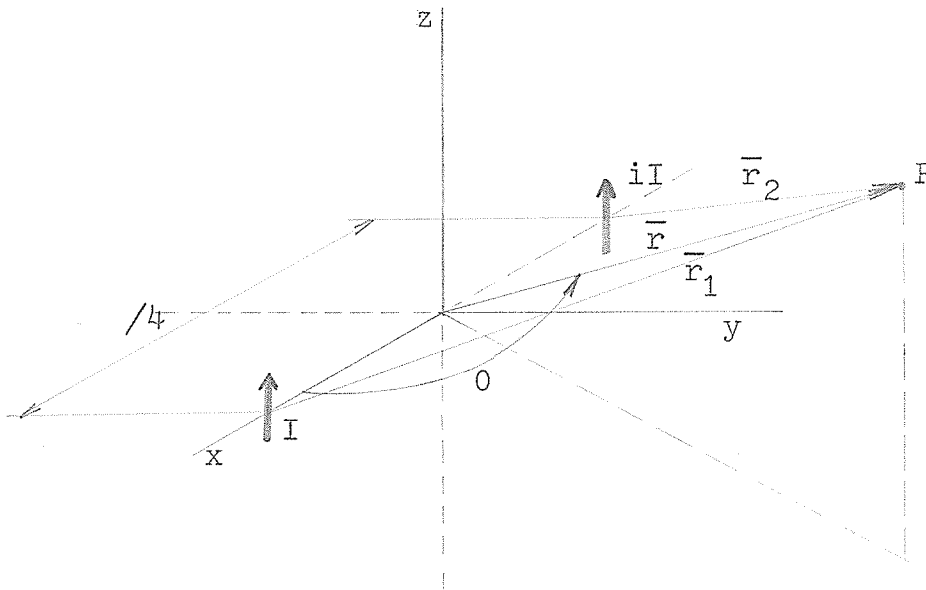


Fig. B - 1

At a point P at a large distance from the antenna the field vectors due to each element are equal in magnitude and have the same direction, but they are out of phase by

$$\alpha = \frac{\pi}{2} + \frac{2\pi}{\lambda} \Delta r \tag{B - 1}$$

where $\Delta r = |\bar{r}_1 - \bar{r}_2|$

The total field at P can be found by a superposition of the field vectors of the individual elements. Since the vectors are out of phase by the angle α , the total field is proportional to $2 \cos(\alpha/2)$. The elements are arranged to be parallel to the z - axis. Hence

$$E_r = E_\phi = H_r = H_\theta = 0$$

$$E_\theta = \frac{A}{r} \sin\theta \cos\left(\frac{\alpha}{2}\right) \exp(-ikr) \quad (\text{B} - 2)$$

$$H = \frac{1}{\eta} E_\theta$$

Now

$$\Delta r \approx \frac{\lambda}{4} \cos\psi = \frac{\lambda}{4} \sin\theta \cos\phi$$

Therefore,

$$\alpha = \frac{\pi}{2} (1 + \sin\theta \cos\phi) \quad (\text{B} - 3)$$

The field is now:

$$E_\theta = \frac{A}{r} \sin\theta \cos\left[\frac{\pi}{4}(1 + \sin\theta \cos\phi)\right] \exp(-ikr) \quad (\text{B} - 4)$$

The force acting on the antenna is given by:

$$\bar{F} = - \frac{1}{2c} \operatorname{Re} \int_S \bar{E} \times \bar{H} \, dS = - \frac{1}{2c} \operatorname{Re} \int_S \bar{a}_r \frac{E_\theta}{\eta} E_\theta^* \, dS$$

or, in the spherical components:

$$F_r = - \frac{A^2}{2c} \int_S \frac{\sin^2 \theta}{r^2} \cos^2 \left[\frac{\pi}{4} (1 + \sin \theta \cos \phi) \right] \, dS \quad (\text{B - 5})$$

$$F_\theta = F_\phi = 0$$

Decomposition of F_r to x and y components gives:

$$F_x = \frac{3P}{8\pi c} \int_0^{2\pi} \int_0^\pi \sin^4 \theta \cos \phi \sin \left(\frac{\pi}{2} \sin \theta \cos \phi \right) \, d\theta \, d\phi \quad (\text{B - 6})$$

$$F_y = 0$$

where P is the radiated power.

The double integral in (B - 6) is evaluated by expanding the term

$$\sin \left(\frac{\pi}{2} \sin \theta \cos \phi \right)$$

in infinite series and integrating term by term. Hence

$$\int_0^{2\pi} \int_0^{\pi} \sin^4 \theta \cos \phi \sin\left(\frac{\pi}{2} \sin \theta \cos \phi\right) d\theta d\phi = \frac{8\pi^2}{15} - \frac{\pi^4}{70} + \frac{\pi^6}{7560} - \dots \quad (\text{B} - 7)$$

The sum of first six terms gives an approximate value 3.9905.

If we substitute this in eq. (B - 6), force acting on the antenna is found as

$$F_x = 0.476 \frac{P}{c} \quad (\text{B} - 8)$$

Imagine now that the point of reference is not on the line connecting the two dipoles, but shifted by a distance d in the negative y - direction (see fig. B - 2).

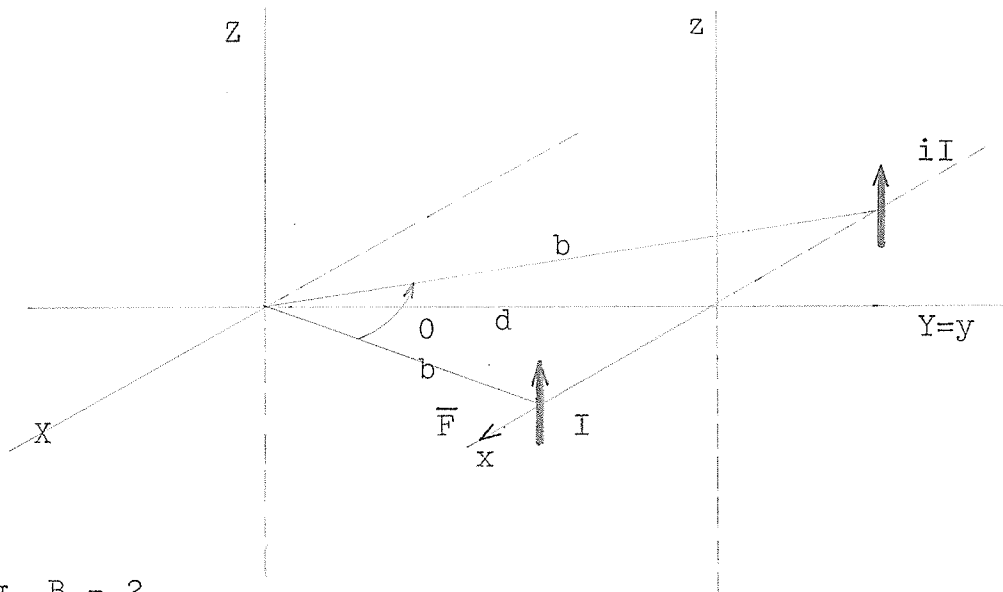


Fig. B - 2

The torque produced in this manner is:

$$T = F_x b \cos \frac{\phi_0}{2} = 0.476 \frac{Pb}{c} \cos \frac{\phi_0}{2} \quad (\text{B} - 9)$$

REFERENCES

- (1) Maxwell, J. C., A Treatise on Electricity and Magnetism, third edition, Dover Publications Inc.
- (2) Lebedev, P., An Experimental Investigation of the Pressure of Light, Astrophysical Journal, vol. 15, p. 60, (1902)
- (3) Nichols, E. F. and Hull, G. F., Pressure due to Light and Heat Radiation, Astrophysical Journal, vol. 15, p. 62, (1902)
- (4) Beth, R. A., Mechanical Detection and Measurement of the Angular Momentum of Light, Physical Review, vol. 50, p. 115, (1936)
- (5) Cullen, A. L., Radiation Pressure of Centimeter Waves, Proc. IEE, vol. 99, p. 100, (1952)
- (6) Bruscaiglioni, P.; Consortini, A. and G. Toraldo di Francia, Electromagnetic Control of the Attitude of Space Vehicles, Alta Frequenza, vol. 32, No. 11, p. 768, (1963)
- (7) Chute, F. S., The Possibility of Stabilizing a Space Vehicle Using Electromagnetic Angular Momentum, PhD dissertation, University of Alberta, January 1966
- (8) Stratton, J.A., Electromagnetic Theory, McGraw - Hill Book Co., New York, (1941)
- (9) Carrara, N., Torque and Angular Momentum of Centimeter Electromagnetic Waves, Nature, vol. 163, p. 882, (1949)

- (10) Harrington, R. F., Time - Harmonic Electromagnetic Fields, McGraw - Hill Book Co., New York, (1961)
- (11) Carrara, N. and Lombardini, P., Radiation Pressure of Centimeter Waves, Nature, vol. 163, p. 171, (1949)
- (12) Jones, D. S., The Theory of Electromagnetism, The MacMillan Co., New York, (1964)